High-order Harmonic Generation and Dynamic Localization in a driven two-level system, a non-perturbative solution using the Floquet-Green formalism

D.F. Martinez

Max-Planck-Institut für Physik komplexer Systeme, Nöthnitzer Straße 38, Dresden 01187

We apply the Floquet-Green operator formalism to the case of a harmonically-driven two-level system. We derive exact expressions for the quasi-energies and the components of the Floquet eigenstates with the use of continued fractions. We study the avoided crossings structure of the quasi-energies as a function of the strength of the driving field and give an interpretation in terms of resonant multi-photon processes. From the Floquet eigenstates we obtain the time-evolution operator. Using this operator we study Dynamic Localization and High-order Harmonic Generation in the non-perturbative regime.

I. INTRODUCTION

The driven two-level system is a particularly important model in physics, since it has proved to be very useful in describing many aspects of the interaction of matter with an electromagnetic field. In the field of atomic physics, this system was traditionally studied using the Rotating Wave Approximation (RWA)[1], in which the counter-rotating term of the harmonic driving is neglected. This approximation is valid only for amplitudes of the driving field that are small compared to the energy difference between the atomic states most affected by the driving field. This was typical for experiments until the 1960's. Presently, technical improvements in laser technology allow experimenters to produce very strong electromagnetic fields (laser pulses) which can produce interesting non-linear effects in their interaction with matter.

The excitation of a spin $1/2$ atom or electron in a magnetic field interacting with a microwave field is another example where the strength of the driving field (RF radiation) can not be assumed to be small.

Also, due to the progress in lithographic techniques and tunable lasers in the terahertz domain, it has become possible to construct semiconductor quantum well structures driven by a strong electromagnetic field. In these systems, several interesting results have been obtained, including, coherent suppression of tunneling [also called Dynamic Localization (DL)][2], collapse of mini-bands in super-lattices[3], absolute negative conductance[4,5], photon-assisted tunneling[6] and AC stark effect[7].

The driven two-level system has also been used to describe an atom moving through a Fabry-Pérot cavity.[8] In this system, the strong coupling regime is already accessible both in the microwave and in the visible regime.

In all of the systems mentioned before, where strong fields are involved, the "counter rotating" term in the time-dependent part of the Hamiltonian does contribute significantly. Therefore, different theoretical approaches beyond RWA are required. One such method was first introduced by Autler and Townes[9]. Using Floquet's theorem and continued fractions, they derived a general solution in order to investigate the effect of a radio frequency field on the l-type microwave absorption line of the doublet $J = 2 \rightarrow 1$ of the molecules of gaseous OCS.

Later, Shirley[10] employed Floquet theory to reduce the solution of a periodic time-dependent Hamiltonian to the problem of diagonalization of a time-independent matrix. This matrix was then used to calculate eigenvalues and transition probabilities for a driven two-level system and also to derive higher order (beyond linear RWA) analytic approximations valid in the case of weak driving. Later approaches to this problem, usually within the context of a spin system in a magnetic and a RF field, have involved the use of continued fractions[11,12,13], although the role played by Floquet theory in those approaches (and in particular the role of the quasi-energy) is not clear.

A different kind of analytical expression for the quasi-energy of the system, which does not involve continued fractions was reported by Zhao[14]. It makes use of group theoretical arguments for its derivation and involves the evaluation of complicated infinite sums. Apart from its intrinsic theoretical value, this solution does not provide a practical way to study this system.

There have been a variety of approaches used to obtain approximate analytic expressions. Most of them have been obtained in the high frequency limit[15,16,17], for $\omega \gg \omega_0$ or in the strong field limit[18,19], for $v \gg \hbar\omega$. Here ω refers to the frequency of the driving, ω_0 is the energy difference between the two levels of the unperturbed Hamiltonian and v is the strength of the driving. One of the most interesting features of a system described by these perturbative solutions is that at some specific values of the driving field strength (zeros of the zeroth-order Bessel function) Dynamic Localization (DL) occurs, which in the context of quantum wells means that despite a nonzero tunneling probability between the wells, a system initially prepared in one of the wells will remain in that well indefinitely. A manifestation of DL [also called Coherent Destruction of Tunneling (CDT)] was first found in a tight binding potential with an applied AC electric field.[20] DL in quantum wells was first studied by Großmann el al.[2]

In a paper by Ivanov[21] in which High-order Harmonic Generation (HHG) by diatomic molecular ions is considered, and then more recently in works by Santana et al.[22] and also Delgado and Gomez Llorente[23], analytical expressions in terms of Bessel functions were found, valid in the (perturbative) regime where DL occurs. This regime can be characterized by the condition $\omega_0/\omega \ll 0$ for any v, or $\omega_0/\omega \ll \sqrt{v/\hbar\omega} \gg 1$. We will say that whenever any of these two conditions is satisfied, the system is in the Dynamic Localization Regime (DLR). When that regime is reached, our results converge to the known Bessel-function expressions.

In this work we present a fully developed Floquet-Green formalism for time periodic systems, which we then use to derive an exact solution for the two level system with harmonic driving. This exact solution is expressed in terms of continued fractions, suitable to the study of the regime where neither the RWA nor any other perturbative approach works. Our aim is to present a whole picture of this system, of its eigenvalues and eigenstates in the different regions of its parameter space and to obtain from the general solution a better understanding of the two main features of this system, namely, Dynamic Localization (DL) and High-0rder Harmonic Generation (HHG).

In section II we derive the Floquet-Green operator formalism and establish a connection between the poles of this operator and the components of the Floquet eigenstates.

In section III we apply this formalism to the specific case of the two-state system with harmonic driving. By making use of continued fractions, we obtain an expression for the quasi-energies. We study the structure of avoided-crossings in the quasi-energies and interpret them in terms of multi-photon processes. We also derive here the Floquet eigenstates (FES) of the system and study their dependence on the amplitude of the driving field for different values of the two-level energy difference. The time-evolution operator is constructed using the FES.

In section IV, using the above mentioned operator, we study Dynamic Localization (DL), and in section V we study High-order Harmonic Generation (HHG).

In Section VI we summarize our findings and give some concluding remarks.

II. FLOQUET-GREEN OPERATOR FOR HARMONIC DRIVING

The pioneering work of Shirley[10] and Sambe[24] laid down the theoretical foundations for a complete treatment of time-periodic potentials, based on the same mathematical tools already developed for time-independent potentials. Of great importance among these tools is the Green's function, whose definition and application for time-periodic systems has not been clear until recently. A Floquet-Green function method for the solution of radiative electron scattering in a strong laser field was introduced by Faisal[25]. In this work we present a fully developed picture of the Floquet-Green's operator formalism for general time-harmonic Hamiltonians that was introduced by the author in a previous work[26], and apply it to the case of a two-state system with harmonic driving.

We start by considering a Hamiltonian of the general form:

$$H(t) = H_0 + 2V\cos(\omega t), \tag{1}$$

were H_0 and V are Hermitian operators in the Hilbert space ($\mathcal{H}$) of the system. Because of the periodicity of the Hamiltonian, according to Floquet's theorem, the solutions to Schrodinger's equation $i\hbar\frac{\partial}{\partial t}|\Psi(t)\rangle = H(x,t)|\Psi(t)\rangle$ are of the form

$$|\Psi^e(t)\rangle = e^{-iet/\hbar}|\phi^e(t)\rangle, \tag{2}$$

where $|\phi^e(t)\rangle = |\phi^e(t + \frac{2\pi}{\omega})\rangle$.

Inserting this into Schrodinger's equation one arrives at the eigenvalue equation

$$H^F(t)|\phi^e(t)\rangle = e|\phi^e(t)\rangle, \tag{3}$$

where $H^F(t)$ is defined as

$$H^F(t) \equiv H(t) - i\hbar\frac{\partial}{\partial t}. \tag{4}$$

As pointed out by Sambe[24], since Eq.(3) is an eigenvalue equation, it can be solved using the standard techniques developed for time-independent Hamiltonians, provided we extend the Hilbert space to include the space of time-periodic functions. In this extended space, the time parameter can be treated as another degree of freedom of the system. A similar concept is used in classical mechanics, and gives rise to the concept of a "half" degree of freedom when dealing with time dependent Hamiltonians.

A suitable basis for this extended Hilbert space ($\mathcal{R}$) is $\{|\alpha\rangle \otimes |n\rangle, ...\}$, where $\{|\alpha\rangle, ..\}$ is a basis for the Hilbert space $\mathcal{H}$ of the system, and we define $\langle t|n\rangle = e^{-in\omega t}$, with n integer. Clearly $\{|n\rangle, ..\}$ spans the vector space ($\mathcal{T}$ of periodic functions, and therefore, $\mathcal{R} = \mathcal{H} \bigotimes \mathcal{T}$. In this basis, Eq.(3) becomes a matrix eigenvalue equation of infinite dimension with an infinite number of eigenvalues. It is not difficult to proof that if e_i is an eigenvalue, with corresponding eigenvector $|\phi^{e_i}(t)\rangle$, then $e_i + m$ is also an eigenvalue (all quantities are assumed to be in units of $\hbar\omega$), with corresponding eigenvector $|\phi^{e_i+m}(t)\rangle = e^{im\omega t}|\phi^{e_i}(t)\rangle$. Accordingly, the eigenstate corresponding to eigenvalue $e_i + m$ has the same structure than the eigenstate corresponding to e_i, except that it is displaced by m on the energy axis. Because of this, to find all the eigenvectors and eigenvalues of the Floquet Hamiltonian one needs only to consider $-\frac{1}{2} \leq e < \frac{1}{2}$. We will use the letter ε to refer to the Floquet eigenvalues restricted to this interval and call them "quasi-energies". Clearly, any Floquet eigenvalue e_i can be written as $e_i = \varepsilon_i + p$ for some $-\frac{1}{2} \leq \varepsilon_i < \frac{1}{2}$ and some integer p. It can be shown that, in general, there are N distinct quasi-energies (except for accidental degeneracies) if the Hilbert space $\mathcal{H}$ is N dimensional.

This periodic structure in the eigenvalues does not mean that the "replica" eigenstates have no relevance; they are also valid solutions of Eq. (3) and are essential for completeness in the extended Hilbert space $\mathcal{R}$[27]. They also allow us to understand some features of the quasi-energies of the system in terms of avoided crossings between "replica" eigenstates.

The Floquet-Green operator for the Floquet Hamiltonian in Eq. (3), is defined by the equation[26],

$$[\mathbf{1}E - H^F(t')]\mathcal{G}(E, t', t") = \mathbf{1}\delta_\tau(t' - t'') \quad , \tag{5}$$

where $\delta_\tau(t)$ is the τ-periodic delta function ($\tau = \frac{2\pi}{\omega}$).

In terms of the complete (infinite) set $\{|\phi^{e_i}(t)\rangle\}$ of eigenfunctions of the Floquet-Hamiltonian (Eq.4), the solution for Eq.(5) is

$$\mathcal{G}(E, t', t'') = \sum_i \frac{|\phi^{e_i}(t')\rangle\langle\phi^{e_i}(t'')|}{E - e_i} \quad . \tag{6}$$

From the previous discussion about the eigenvalues and eigenfunctions of the Floquet Hamiltonian, we can write the Floquet-Green operator entirely in terms of the eigenfunctions corresponding to values e_i between $-\frac{1}{2}$ and $\frac{1}{2}$. We will denote these eigenvalues as ε_γ. Using this, the Floquet-Green operator can be written as

$$\mathcal{G}(E, t', t'') = \sum_\gamma \sum_p e^{ip\omega(t'-t'')} \frac{|\phi^{\varepsilon_\gamma}(t')\rangle\langle\phi^{\varepsilon_\gamma}(t'')|}{E - \varepsilon_\gamma - p} \quad , \tag{7}$$

where $\gamma = 1, ...N$ for $\mathcal{H}$ being N-dimensional, and $p = -\infty, ..., \infty$.

Operating on both sides of this equation with $\frac{1}{\tau^2}\int_0^\tau \int_0^\tau e^{im\omega t'} e^{-in\omega t''} dt'' dt'$ we obtain

$$\mathcal{G}_{m,n}(E) = \sum_{\gamma,p} \frac{1}{E - \varepsilon_\gamma - p}|\phi^{\varepsilon_\gamma}_{m+p}\rangle\langle\phi^{\varepsilon_\gamma}_{n+p}|, \tag{8}$$

where

$$\mathcal{G}_{m,n}(E) = \frac{1}{\tau^2}\int_0^\tau \int_0^\tau e^{im\omega t'} e^{-in\omega t''} \mathcal{G}(E, t', t'') dt'' dt' \quad ,$$

and

$$|\phi^{\varepsilon_\gamma}_m\rangle = \frac{1}{\tau}\int_0^\tau e^{im\omega t'}|\phi^\varepsilon(t')\rangle dt'. \tag{9}$$

For $m = n = 0$,

$$\mathcal{G}_{0,0}(E) = \sum_{\gamma,p} \frac{1}{E - \varepsilon_\gamma - p}|\phi^{\varepsilon_\gamma}_p\rangle\langle\phi^{\varepsilon_\gamma}_p| \quad . \tag{10}$$

This last equation shows us the relationship between the residue of the operator $\mathcal{G}_{0,0}(E)$ at the pole $\varepsilon_\gamma + p$ and the Fourier component $|\phi^{\varepsilon_\gamma}_p\rangle$ of the Floquet eigenstate $|\phi^{\varepsilon_\gamma}(t)\rangle$. Notice that $|\phi^{\varepsilon_\gamma}(t)\rangle = \sum_p e^{-ip\omega t}|\phi^{\varepsilon_\gamma}_p\rangle$. From this we

conclude that, *corresponding to each pole at $E = \varepsilon_\gamma + p$ of the Floquet-Green operator $\mathcal{G}_{0,0}(E)$ there is an oscillating term of the form $e^{-ip\omega t}$ in the Floquet eigenstate specified by the quasi-energy ε_γ.*

Let us go back to the task of finding an explicit solution to the Floquet-Green operator in Eq.(5). Applying $\frac{1}{\tau}\int_0^\tau \int_0^\tau e^{im\omega t'}e^{-in\omega t''}dt''dt'$ on both sides of this equation, and using Eq.(4) together with the definitions above we get

$$[\mathbb{1}(E+m) - H_0]\mathcal{G}_{m,n} - V(\mathcal{G}_{m+1,n} + \mathcal{G}_{m-1,n}) = \mathbb{1}\delta_{m,n} \tag{11}$$

The explicit solution of this equation, in terms of matrix continued fractions follows from[26]. The resulting expression for the operator $\mathcal{G}_{0,0}(E)$ is

$$\mathcal{G}_{0,0}(E) = (\mathbb{1}E - H_0 - V_{\text{eff}}(E))^{-1}, \tag{12}$$

where

$$V_{\text{eff}}(E) = V_{\text{eff}}^+(E) + V_{\text{eff}}^-(E) \quad,$$

with

$$V_{\text{eff}}^\pm(E) = V\cfrac{1}{E \pm 1 - H_0 - V\cfrac{1}{E \pm 2 - H_0 - V\cfrac{1}{\vdots}V}V}V \quad, \tag{13}$$

We now specialize this result for the case of a two state system driven by a classical single frequency potential.

III. HARMONICALLY DRIVEN TWO-LEVEL SYSTEM

In this section we apply the formalism previously presented to the case of a driven two-level system of the form

$$H = \frac{\tilde{\omega}_0}{2}\sigma_z + 2v\cos(\omega t)\sigma_x \quad, \tag{14}$$

where H, $\tilde{\omega}_0$ and v are given in units of $\hbar\omega$. In the context of an electron interacting with an electric field, the amplitude $2v$ corresponds to the (static) dipole moment of the electron times the applied electric field, i.e. $2v = \mu E_0/\hbar\omega$, (the factor of two has been introduced for convenience) and the classical electric field is of the form $E(t) = E_0\cos(\omega t)$. In a double quantum-dot realization of this Hamiltonian, the non-driven part, $\frac{\tilde{\omega}_0}{2}\sigma_z$, describes the tunneling between the states localized on each dot, $\{|1\rangle, |2\rangle\}$. This tunneling gives rise to a splitting of $\hbar\omega_0 = \tilde{\omega}_0\hbar\omega$ between the energy levels $-\frac{\hbar\omega_0}{2}, +\frac{\hbar\omega_0}{2}$, whose corresponding eigenstates we denote by $\{|a\rangle, |b\rangle\}$, and where $|b\rangle = \frac{1}{\sqrt{2}}(|1\rangle + |2\rangle)$, and $|a\rangle = \frac{1}{\sqrt{2}}(|1\rangle - |2\rangle)$. The Hamiltonian in Eq.(14) is written in the basis $\{|a\rangle, |b\rangle\}$. For an atomic system, $\frac{\tilde{\omega}_0}{2}\sigma_z$ describes two bound states of the atomic (or molecular) potential, or, in the context of ionizing systems it could also be thought of as describing a bound state and the continuum[28,29]. An electron moving in a Fabry-Pérot cavity[8] or a $1/2$ spin system with an applied magnetic and microwave field[11,12,13], are also examples of systems where this model has been used.

Continued fractions methods have been used before to study this system, specially in the context of spin $1/2$ systems in a magnetic and RF field, starting with the seminal work of Autler and Townes[9]. Also, a previous treatment of this problem where the time dependent Green's function and continued fractions were used, although without reference to the Floquet formalism can be found in the work by Gush and Gush[30]. There have been several perturbative approaches to this problem, as it was mentioned before. Here, we will focus on the properties of the exact solution, and in particular we will study its dependence on the strength of the driving field and the connection with HHG and DL.

To find the exact solution to this Hamiltonian we need to evaluate Eqs. (12,13), for the case $V = v\sigma_x$ and $H_0 = \frac{\omega_0}{2}\sigma_z$. It can be checked easily that, given the off-diagonal form of V and the diagonal form of H_0, the matrices $V_{\text{eff}}^\pm(E)$ are diagonal. Its diagonal components will be denoted respectively by $\{v_a^\pm(E), v_b^\pm(E)\}$. The dynamic effective-potential $V_{\text{eff}}(E)$ is therefore also diagonal and of the form

$$V_{\text{eff}}(E) = \begin{bmatrix} v_a^+(E) + v_a^-(E) & 0 \\ 0 & v_b^+(E) + v_b^-(E) \end{bmatrix}. \tag{15}$$

The $v_{a/b}^{\pm}$ functions are given by the following coupled recursive relations

$$v_a^{\pm}(E) = \frac{v^2}{E \pm 1 - \frac{\tilde{\omega}_0}{2} - v_b^{\pm}(E \pm 1)}, \quad v_b^{\pm}(E) = \frac{v^2}{E \pm 1 + \frac{\tilde{\omega}_0}{2} - v_a^{\pm}(E \pm 1)}. \tag{16}$$

Replacing $v_a^{\pm}$ into $v_b^{\pm}$ (and vice versa) we obtain the de-coupled recursive relations

$$v_a^{\pm}(E) = \cfrac{v^2}{E \pm 1 - \cfrac{\tilde{\omega}_0}{2} - \cfrac{v^2}{E \pm 2 + \cfrac{\tilde{\omega}_0}{2} - v_a^+(E \pm 2)}} \quad , \qquad v_b^{\pm}(E) = \cfrac{v^2}{E \pm 1 + \cfrac{\tilde{\omega}_0}{2} - \cfrac{v^2}{E \pm 2 - \cfrac{\tilde{\omega}_0}{2} - v_b^+(E \pm 2)}}. \tag{17}$$

From Eq.(12), the solution for $\mathcal{G}_{0,0}(E)$ is also a diagonal matrix of the form

$$\mathcal{G}_{0,0}(E) = \begin{bmatrix} g^a(E) & 0 \\ 0 & g^b(E) \end{bmatrix}, \tag{18}$$

with

$$g^a(E) = \frac{1}{E + \frac{\tilde{\omega}_0}{2} - v_a^+(E) - v_a^-(E)} \quad , \tag{}$$

$$g^b(E) = \frac{1}{E - \frac{\tilde{\omega}_0}{2} - v_b^+(E) - v_b^-(E)} \quad . \tag{19}$$

It can easily be seen from Eq.(17) that this system possesses the symmetry $v_a^{\pm}(-E) = -v_b^{\mp}(E)$, which from Eq.(19) gives us $g_a(-E) = -g_b(E)$. This means that to find the two quasi-energies of the system one only has to look for a pole in either $g_a(E)$ or $g_b(E)$ in the range $-0.5 \leq E \leq 0.5$; the other pole is symmetrically located on the opposite side of the (quasi) energy axis.

A. Poles of $\mathcal{G}_{0,0}(E)$ and the quasi-energies of the system

As discussed before, the quasi-energies of the system can be obtained from the poles in $g_a(E)$ and $g_b(E)$. We showed that it is sufficient to study the poles in only one of these functions since for any pole in $g_a(E)$ at $E = E^*$ there is a corresponding pole in $g_b(E)$ at $E = -E^*$. This implies the existence of two quasi-energies in the system, $\varepsilon, -\varepsilon$. The quasi-energy ε can be obtained from the solution to $g_b(E)^{-1} = 0$ in the interval $-0.5 < E < 0.5$. From Eqs. (17),(19), the poles of $g_b(E)$ satisfy the equation,

$$\delta = \cfrac{v^2}{wo - \cfrac{v^2}{\delta + 2 - \cfrac{v^2}{\delta + 3 + \tilde{\omega}_0 - \cfrac{v^2}{\delta + 4 - \cfrac{v^2}{\vdots}}}}} + \cfrac{v^2}{\delta - 1 + \tilde{\omega}_0 - \cfrac{v^2}{\delta - 2 - \cfrac{v^2}{\delta - 3 + \tilde{\omega}_0 - \cfrac{v^2}{\delta - 4 - \cfrac{v^2}{\vdots}}}}}, \tag{20}$$

where $\delta = E - \frac{\tilde{\omega}_0}{2}$. The quasi-energy is obtained as $\varepsilon = (\frac{\tilde{\omega}_0}{2} + \delta) \bmod 1$.

In Fig. 1 we show one of the quasi-energies of the system, for different values of $\tilde{\omega}_0$. These functions are plotted as a function of the driving strength v. We have included the resonant case $\tilde{\omega}_0 = 1$ and several values in the high frequency regime where $\tilde{\omega}_0 < 1$. In the limit when $\tilde{\omega}_0 << max(1, \sqrt{v})$, the function $\varepsilon(v) \approx \frac{\tilde{\omega}_0}{2} J_0(4v)$. This result was first obtained by Shirley[10]. It is precisely in this regime where it was shown[22,23] that DL appears as a dominant feature. As $\tilde{\omega}_0$ decreases we observe a very quick convergence to the approximate result $\varepsilon(v) \approx \frac{\tilde{\omega}_0}{2} J_0(4v)$. Already for $\tilde{\omega}_0 = 0.25$, the difference between the exact result for $\varepsilon(v)$ and the approximation cannot be observed at the scale of the graph. For $\tilde{\omega}_0 = 0.1$ we plotted both $\varepsilon(v)$ and $-\varepsilon(v)$ to make the location of the zeros of $J_0(4v)$ more visible.

As we can also see in Fig.2, increasing $\tilde{\omega}_0$ always displaces the zeros of $\varepsilon(v)$ towards smaller values. This behavior was also observed by Villas-Bôas et al.[31] in the case of a double quantum well with an intense AC electric field and an applied magnetic field. Notice also that, as it is easy to derive analytically, the only case when the initial slope of the quasi-energy is not zero is for the resonant case.[32]

In Fig. 2 we show the quasi-energy as a function of the driving strength v, for low frequencies, where $\tilde{\omega}_0 \geq 1$. The resonant case is included for comparison. Also, the dotted line shows the functions $\pm 0.05 J_0(4V)$ in order to indicate the location of the zeros of this Bessel function. As one increases $\tilde{\omega}_0$, the amplitude and sharpness of the oscillations around $\varepsilon = 0$ increases, the location of the zeros shifts to the left, and the parabola that describes (except in the resonant case) the initial behavior of the curve opens up. For $\tilde{\omega}_0 \gtrsim 2$ one can get from Eq.(20) that the initial behavior of the quasi-energy is parabolic and has the form

$$\delta(v) \approx \frac{2\tilde{\omega}_0}{\tilde{\omega}_0^2 - 1} v^2 \tag{21}$$

This remains a good approximation for all values of v until $\delta(v) \approx \frac{\tilde{\omega}_0 - 1}{4}$, and provided $\epsilon(v)$ does not reach the edges of the Brillouin zone (-0.5,0.5) before that. If it does so, then, the quasi-energy experiences an avoided crossing, whose sharpness is proportional to $\tilde{\omega}_0$ and decreases with the value of v at which the anti-crossing occurs.

B. Avoided crossings

In Fig.3 we can see that the structure of the quasi-energy is determined by a regular sequence of avoided crossings which get broader as the strength of the driving field v is increased (resonant case shown in the figure).

Let us consider the first avoided crossings, the ones along the line marked "3 ph. res" in Fig. 3. To zero order in v, the eigenvalues and eigenvectors of the Floquet-Hamiltonian are the state vectors $|a\rangle|n\rangle, |b\rangle|n\rangle$, for any integer n. In this basis, the time-dependent potential can be written as $V = v\sigma_x(a + a^\dagger)$. When the effect of one photon processes (in the RWA) is included, one obtains that the new set of eigenstates is $\{|n, \pm\rangle\}$, for any integer n, and where $|n, \pm\rangle = \frac{1}{\sqrt{2}}(|a\rangle|n\rangle \pm |b\rangle|n-1\rangle)$. It's corresponding eigenvalues are $e_n^\pm = \mp\frac{1}{2} + n \pm v$. This one photon process is in a sense an avoided crossing, with a width that goes to zero as $v \to 0$. One can see that, near $v \approx 1$, the eigenvalues corresponding to the eigenstates $|n, \pm\rangle$ and $|n \pm 2, \mp\rangle$ would cross if only fist order processes where allowed. To second order this degeneracy is not lifted since $\langle n \pm 2, \mp|V^2|n, \pm\rangle = 0$. Only when third order processes are included, this degeneracy is lifted, since it is easy to check that $\langle n \pm 2, \mp|V^3|n\pm\rangle \neq 0$. Third order processes are therefore involved in the avoided crossings near $v \approx 1$.

For the resonant case, after the first avoided crossing ($v \approx 1$), for example between the states $|1, -\rangle$ and $|-1, +\rangle$, and because of considerable overlap between the 3 photon resonance and the 5 photon resonance, this states do not completely exchange their identities, as it would be the case in a well isolated avoided crossing. An "identity exchange" between Floquet states can clearly be observed for values of $\tilde{\omega}_0$ and v for which there is a sharp avoided crossing (i.e. $\tilde{\omega}_0 = 3.0$ in Fig.5). In Fig.3, for the resonant case we can see that even though the structure of the eigenstates after the first avoided crossing is not necessarily of the form $|n\rangle\rangle$, the points where the quasi-energies of these "first-order" FES cross, come close to the actual location of the avoided crossings. This is an indication that those states are dominant in the structure of the eigenstates, a fact that can be checked by comparing the actual structure of the FES in Fig. 6, at some amplitude v, with the corresponding "first order" FES eigenvalues that intersect at the closest avoided crossing in Fig. 3. For $v \approx 5$ the peak components in the FES are only one unit of energy further out that the expected value from the simple picture in Fig.3. It is an interesting feature of this system the fact that the FES obtained for small driving amplitudes constitute the "bare bones" structure of the FES and to a good extent they determine the avoided crossings structure of the quasi-energies (at least for a larger-than-expected range of driving field amplitudes).

This avoided crossings structure, to a certain approximation, can be thought of as mostly due to odd-photon processes between FES. Even more, we will argue that at least for a range of v ($0 < v \lesssim 4$ for the resonant case), the main contribution to the avoided crossings is a three photon process for the first avoided crossing, 5 photon for the second avoided crossing, and so on (in the resonant case). For any value of $\tilde{\omega}_0$ we find that the number of photons involved in the first resonance depends on the initial distance between the two unperturbed levels ($\tilde{\omega}_0$). If for example $\tilde{\omega}_0 = 3$ the first avoided crossing will be the 5 photon resonance (Fig.5); for $\tilde{\omega}_0 = 5$ it will be the 7 photon resonance, etc. In general we can write that, for $\tilde{\omega}_0 \geq 1$ the order of the first resonance is $2 \operatorname{Int}(\frac{\tilde{\omega}_0 - 1}{2}) + 3$. The avoided crossings picture holds for any $\tilde{\omega}_0$ provided v is not too big; an estimate is $v \lesssim 4\tilde{\omega}_0^2$. Above this, the overlap between different photon processes is too big for our simple picture to apply.

In Fig.3. it can be seen that the states that intervene at each avoided crossing are of the form $|2n + 1, -\rangle$ and

$|2n + 1 - 2m, +\rangle$, for $m = 1, 2, 3....$ It is easy to check that

$$\langle 2n + 1, -|V^q|2n + 1 - 2m, +\rangle \neq 0, \quad \text{only for} \quad q = 2m - 1, 2m + 1, ...$$

This is a good indication that these avoided crossings can be interpreted as multi-photon resonances that involve odd numbers of photons. From Fig. 3, we see that at the avoided crossing A, from the interacting states $|1, -\rangle$ and $|-1, +\rangle$, there should be a three photon exchange between $|a\rangle|1\rangle$ and $|b\rangle| - 2\rangle$ and a 1 photon exchange between $|a\rangle| - 1\rangle$ and $|b\rangle|0\rangle$. From the exact result for the components of one of the FES shown in Fig. 6 we see that the dominant component before the crossing is $|a\rangle|1\rangle$ and therefore, at $v = 1$ (which is near the crossing), the two dominant components should be $|a\rangle|1\rangle$ and $|b\rangle| - 2\rangle$; this corresponds to a three photon process. Near the avoided crossing B in Fig.3, where $v \sim 2$, we can see from Fig.5 that the dominant components are $|a, 3\rangle$ and $|b, -2\rangle$ which corresponds to a 5 photon exchange. For values of $\tilde{\omega}_0$ and v for which the avoided crossings are sharper one gets an even clearer picture of those avoided crossing as resulting from the exchange of a specific odd number of photons between Floquet states.

It is interesting to see how this description of avoided crossings and photon processes is reflected by the structure of the continued fractions in Eq.(20) and how the different terms in it contribute to the features of the quasi-energy as a function of the driving amplitude. From examination of Eq.(20) it is not difficult to see that for small v, each term of the form $\delta + \alpha$ gives a solution near $\delta = -\alpha$. To find accurately the solution of δ for a particular value of v one does not need to (nor can) include an infinite number of terms in the C.F. An important question is therefore, how many terms to include and why? To study this, we first propose a way to truncate Eq.(20) so that we obtain, in each case, a symmetrical set of solutions. For illustration we will continue focusing on the particular case of resonance ($\tilde{\omega}_0 = 1$), as it is straight forward to apply the same ideas shown here for other values of $\tilde{\omega}_0$.

Eq.(20) can be put in the form

$$F^+(E)F^-(E) = v^2, \tag{22}$$

with

$$F^+(E) = \delta - \cfrac{v^2}{\delta + 1 + \tilde{\omega}_0 - \cfrac{v^2}{\delta + 2 - \cfrac{v^2}{\delta + 3 + \tilde{\omega}_0 - \cfrac{v^2}{\vdots}}}} \quad , \quad F^-(E) = \delta - 1 + \tilde{\omega}_0 - \cfrac{v^2}{\delta - 2 - \cfrac{v^2}{\delta - 3 + \tilde{\omega}_0 - \cfrac{v^2}{\delta - 4 - \cfrac{v^2}{\vdots}}}}. \tag{23}$$

To understand the effect of the different terms in the C.F. we will truncate the functions $F^\pm$ at different levels and plot the solutions for δ. $F_n^\pm$ refers to the truncated version of $F^\pm$ where v^2 appears n times[33], i.e.

$$F_0^+ = \delta, \quad F_1^+ = \delta - \frac{v^2}{\delta + 1 + \tilde{\omega}_0}, \quad F_2^+ = \delta - \cfrac{v^2}{\delta + 1 + \tilde{\omega}_0 - \cfrac{v^2}{\delta + 2}}, \quad .... ,$$

and likewise for F_n^-.

In the different panels in Fig. 4 we plot the solutions for $\delta(v)$ as obtained from the equation $F_n^+ F_n^- = v^2$ for $n = 0, 1, 2, 3$ [panels a) through d)], and only for the resonant case $\tilde{\omega}_0 = 1$. We also plot with a dashed line and for comparison, the exact result for δ (only the two smallest roots are shown). Also, in front of each plot there is an insert with a diagram with lines and arrows. The lines represent each term that has been included in the continued fractions F_n^+ and F_n^-. As we mentioned before, each term of the form $\delta + \alpha$ contributes with an eigenvalue curve that originates at $\delta = -\alpha$. There are two kinds of terms of that form in the C.F.'s of Eq.(20): $\delta \pm 2n$ and $\delta + \tilde{\omega}_0 \pm (2m + 1)$. The first ones contribute, at $v = 0$, with a solution at $\delta = \mp 2n$ and therefore a pole at $E = E_b \mp 2n$. The second kind gives a solution for $\delta = -\tilde{\omega}_0 \mp (2m + 1)$ which contributes with a pole at $E = E_b - \tilde{\omega}_0 \mp (2m + 1) = E_a \mp (2m + 1)$. To the lines on the left we associate the states $|a, 2n + 1\rangle$. We will label this lines as $a + 2n + 1$, for some n; the lines on the right we associate with the particle-field states $|b, 2n\rangle$ and label them as $b + 2n$. A similar picture would result from studying the poles of $g_a(E)$.

When two such terms in the CF are included, then we see, in the corresponding panel in Fig.4, a pair of solutions, which at $v = 0$ converge to $\delta = 2n$ and split for $v > 0$. We know, from previous discussions, that the upper one should correspond to the FES, $|2n + 1, +\rangle = |a, 2n + 1\rangle + |b, 2n\rangle$, and the lower one to $|2n + 1, -\rangle = |a, 2n + 1\rangle - |b, 2n\rangle$. The arrows at the end of the lines show the direction in which the corresponding eigenvalue would move when v is increased. The repulsion between the eigenstates $|2n + 1, \pm\rangle$ is due to the exchange of one photon between $|a\rangle$ and

$|b\rangle$. This is the main process at work in panels a) and b). In panel c) two new processes enter the picture: As the levels move apart due to the one photon resonance, another resonance (A) can now occur when the levels $|3,-\rangle$ and $|1,+\rangle$ mostly due to the transfer of three photons between $|a,3\rangle$ and $|b,0\rangle$. This process appears for the first time for $F_2^\pm$ when the term $|a,3\rangle$ is included in the CF. A replica of this three photon resonance occurs also between levels $|1,-\rangle$ and $|-1,+\rangle$.

When $|a,3\rangle$ and $|b,-2\rangle$ is included, the second process that becomes available is the five photon resonance between levels $|3,-\rangle$ and $|-1,+\rangle$ (after this level have interacted with $|1,+\rangle$ and $|1,-\rangle$ respectively). This resonance becomes more clearly defined in panel d) where more levels are included. Even though, as compared to c), no new resonances appear in d), the inclusion of levels $|a,-3\rangle$ and $|b,4\rangle$ contributes to sharpen the resonances already visible in c) and in particular the 5 photon resonance B. This shows that, as mentioned before, there are several odd-photon processes that contribute to a particular avoided crossing. There is however, an odd number of photons that seems to contribute the most and without which, if the corresponding levels are not included, the corresponding avoided crossing does not seem to occur. That specific number of photons is shown on the top of Fig.3. For $v > 4$ this pictures begins to falter, and the avoided crossings begin to depend more on a higher number of photons than what would be predicted from Fig.3. For $v = 5$ for example, a better description of the crossing would be for a 15 photon resonant process, not the expected 13. For even higher values of $\tilde{\omega}_0$ this picture holds on a bigger range of the driving field amplitude, namely, for $v \lesssim 4\tilde{\omega}_0^2$. As mentioned before, one can see that in Fig.5, for $\tilde{\omega}_0 = 3$, the first avoided crossing is clearly a 5 photon resonance.

As an empirical rule, which agrees with the above observations, we found that to obtain an accurate result for the quasi-energy up to a value v of the driving potential one needs to use the function $F^n(E)$, with $n > \text{Int}(2v)$.

C.   Components of the Floquet EigenStates

In the previous subsection we showed how to obtain the diagonal part of the Floquet-Green operator and discussed its pole structure and their avoided crossings. In this part we study the Floquet eigenstates and the general behavior of them as the amplitude of the driving field changes. In Appendix A we show that the FES of this system can be written in the form

$$|\phi^{-\varepsilon}(t)\rangle = K(t)|a\rangle \ + \ Z(t)|b\rangle$$

and

$$|\phi^{\varepsilon}(t)\rangle = -Z(t)^*|a\rangle \ + \ K(t)^*|b\rangle, \tag{24}$$

with

$$K(t) = N[\ \sum_{n=-\infty}^{\infty} e^{-2in\omega t}K_{2n}(-\varepsilon)]\ ,$$
$$Z(t) = N[\ \sum_{n=-\infty}^{\infty} e^{-i(2n-1)\omega t}Z_{2n-1}(-\varepsilon)]. \tag{25}$$

N is a normalization constant and $|K(t)|^2 + |Z(t)|^2 = 1$. In appendix A we also show the explicit form of the components K_{2n}, Z_{2n+1}, in Eq.(61). It can there be seen that all components K_{2n} and Z_{2n-1} are real, and therefore $K(0)$ and $Z(0)$ are also real numbers.

In Fig.6 we show the components of one of the Floquet eigenstates of the system, $|\phi^{\varepsilon}(t)\rangle$, for the resonant case, and for eight different values of the driving field amplitude, In the upper figure of each panel we show the quantities Z_n,K_n (with n odd for Z_n and n even for K_n), and in the lower panels we show the quantities $\ln|Z_n|$, $\ln|K_n|$.

A noticeable qualitative difference between the behavior of Z_{2n-1} and K_{2n} is the fact that for stronger values of v, the former becomes more antisymmetric while the last one becomes more symmetrical around $n = 0$. We will comment shortly about the consequence that this has for the dynamic localization of the system. The fact that the eigenstates of the system have components that are harmonics of the driving field frequency ω, translates, as we will study in the next section, into a (coherent) emission spectrum of the system which contains also many frequencies that are multiples of the frequency of the driving field. The possibility of exciting a system at a particular frequency with a strong field, and producing radiation that includes many harmonics of the driving frequency (in some cases even hundreds of them) is called High Harmonic Generation (HHG) and has been studied in many experiments.[34] Driven two-level systems have been studied in the past to understand the general features of HHG such as the

existence of a plateau in the spectrum followed by a sharp cut-off where the amplitudes of the harmonics decrease rapidly.[16,21,28,35,36,37,38]

As one can see directly from Fig. 6 (resonant case), in most of the cases shown, the Floquet eigenstates show a particular structure with two clearly distinguishable regions. The first region which, in a non-rigorous way we call the "chaotic" one, can be described as corresponding to the Floquet components with $|n| \lesssim N_e = 2v - 1$ (for $v \geq 1$ in the resonant case). The amplitude of these Floquet components depends strongly on n and on v, and there are frequent sign changes. This gives rise to the "plateau" region typical in HHG. The second region, or the "regular" one corresponds to the components with $|n| > N_e$, and it is characterized by having amplitudes that decay exponentially with n. Also, notice that the components K_n and Z_n do not change sign in that region, with $K_{2n} > 0$, and $\text{sg}(Z_{2n-1}) = \text{sg}(n)$ in the " regular" region ($\text{sg}(x) \equiv x/|x|$). For other values of $\tilde{\omega}_0$, a plateau region was always found whenever $v \gtrsim \sqrt{\tilde{\omega}_0}$ (for $\tilde{\omega}_0 \geq 1$), in agreement with a similar expression obtained by Kaplan[28] in the limit $\tilde{\omega}_0 >> 1$. For $\tilde{\omega}_0 < 1$, the plateau forms for any $v \gtrsim 1$.

The expression $N_e = 2v - 1$ can be derived in a simple way. First, we look at the conditions to obtain, for $n > 0$ a perfectly flat, triple plateau in the components of the FES. This means that we will assume $K_{n+2} = Z_{n+1} = K_n$ (which gives three consecutive components with the same amplitude), for some n even. This condition can be achieved if, from Eq.(61), $v_a^+(\varepsilon + n) = v_b^+(\varepsilon + n + 1) = v$. From Eq.(16) we get the condition,

$$n = 2v - 1 + \frac{\tilde{\omega}_0}{2} - \varepsilon.$$

If instead, we had chosen the triple plateau to be of the form $Z_{n+2} = K_{n+1} = Z_n$ (for n odd), then, the equation for n would be

$$n = 2v - 1 - \frac{\tilde{\omega}_0}{2} - \varepsilon.$$

If we now apply the same reasoning for a triple cusp to occur in the negative energy components, beginning at the component $-n$, we get the conditions (for n odd and even)

$$n = 2v - 1 + \frac{\tilde{\omega}_0}{2} + \varepsilon,$$

$$n = 2v - 1 - \frac{\tilde{\omega}_0}{2} + \varepsilon.$$

Clearly, since in general this 4 equations can not be (nor we care for them to be) satisfied simultaneously, we look for a condition that will produce a simple (possibly) double cusp, *both* at N_e and $-N_e$. This would describe the location of the two broad peaks that are, in all cases, at the limit between the "chaotic" and the "regular" region. For obtaining this symmetric flat cusp condition we pick the equation that is right in the middle of the set of 4 equations given above. This equation is clearly

$$N_e = 2v - 1, \tag{26}$$

with the nice property that the ε and the $\tilde{\omega}_0$ dependence drops out. This is a result that should work well whenever there is a well defined "plateau" region, that is, for $v \geq \sqrt{\tilde{\omega}_0}$ when $\tilde{\omega}_0 \geq 1$, or $v \geq 1$ when $\tilde{\omega}_0 < 1$. As can be seen in Fig.6, for $\tilde{\omega}_0 = 1$ and $v \geq 1$, this equation seems to describe well the location of the peaks in the spectrum of an eigenstate that separate the plateau from the exponential decay region. For other values of $\tilde{\omega}_0$ it gives also good agreement with the data.

To investigate further the structure of the FES of the system, we use Eq.(24), and evaluate at $t = 0$,

$$
\begin{aligned}
|\phi^{-\varepsilon}(0)\rangle &= \cos\theta|a\rangle + \sin\theta|b\rangle, \\
|\phi^{\ \varepsilon}(0)\rangle &= -\sin\theta|a\rangle + \cos\theta|b\rangle,
\end{aligned}
\tag{27}
$$

and where, using $K(0)^2 + Z(0)^2 = 1$, we have defined the angle θ so that $K(0) = \cos\theta$, and $Z(0) = \sin\theta$.

We now concentrate on the study of the quantities $\cos\theta(v)$, $\sin\theta(v)$, $\theta(v)$, which, as we will see in the next sections, play an important part in the evolution of the system, and correspondingly in the Dynamical Localization and Harmonic Generation of the system. In what follows we will study them for three different values of the parameter $\tilde{\omega}_0$: Driving frequency above resonance, for $\tilde{\omega}_0 = 0.5$; resonant case for $\tilde{\omega}_0 = 1$ and driving frequency below resonance, for $\tilde{\omega}_0 = 2$.

In Figs. 7,8,9, we show the results for $\tilde{\omega}_0 = 0.5$, $\tilde{\omega}_0 = 1.0$ and $\tilde{\omega}_0 = 2.0$ respectively. The upper panels show the dependence of the functions $\cos^2(2\theta(v))$ and $\sin^2(2\theta(v))$, and the lower panel the functions $\theta(v)$ and $\varepsilon(v)$. As a

function of the driving field amplitude v, these functions show an oscillatory behavior, which can be better appreciated in the lower panels, where the function $\theta(v)$ is plotted along side with $\varepsilon(v)$. An interesting feature of this functions is the fact that in general, and to a good approximation, there seems to be a phase shift of $\approx \pi/2$ between $\varepsilon(v)$ and $\theta(v)$, which corresponds to a distance of $\Delta v \approx 0.4$ between their maxima. This means that to (almost) every maxima of $\theta(v)$ corresponds a zero of $\varepsilon(v)$ (the DL points) and vice versa, with the only exceptions occurring at the first maxima or the first zero of this functions. Notice also that $\theta(v)$ does not oscillate symmetrically around zero, with the clear consequence that the peaks in the functions $\cos^2(2\theta(v))$ and $\sin^2(2\theta(v))$ have uneven heights, with alternating high and low peaks, although with an overall decrease in height. This alternating pattern of maxima seems to be a general feature of the system, which we have found for all the values of $\tilde{\omega}_0$ that we examined.

The DL regime, which can be characterized by the parameter $\alpha' \equiv \tilde{\omega}_0 \min(1, 1/\sqrt{v}) << 1$, has been studied in several works. In this regime it was found[16,22] that, at $t = 0$, the eigenstates of the system are of the form

$$
\begin{aligned}
|\phi^{-\varepsilon}(0)\rangle &= |a\rangle \;+\; \tilde{\omega}_0\frac{\pi}{4}H_0(4v)|b\rangle, \\
|\phi^{\;\varepsilon}(0)\rangle &= -\tilde{\omega}_0\frac{\pi}{4}H_0(4v)|a\rangle \;+\; |b\rangle
\end{aligned}
\tag{28}
$$

where $H_0(4v)$ is the Struve function[39] defined as

$$
H_0(4v) \equiv \frac{4}{\pi}\sum_{n=0}^{\infty}\frac{J_{2n+1}(4v)}{2n+1}
\tag{29}
$$

In Figs. 7,8,9, in the lower panel we have plotted with a dash-dot line the function $\tilde{\omega}_0\frac{\pi}{4}H_0(4v)$. As it was expected, since in the DL regime $\sin\theta << 1$, then $\sin\theta \approx \theta$, and $\theta(v) \rightarrow \tilde{\omega}_0\frac{\pi}{4}H_0(4v)$. The convergence of $\theta(v)$ to the Struve function is clearly slower for the bigger values of $\tilde{\omega}_0$. It is however rather remarkable that the Struve function seems to approximate well the function $\theta(v)$ much before the DL regime condition is satisfied ($\alpha \ll 1$); for example, for $\tilde{\omega}_0 = 0.5$, and $v = 1$, or $\tilde{\omega}_0 = 1$ and $v = 4$, which both give $\alpha = 0.5 \lesssim 1$ we already see a good agreement between those two functions. One can also see from Fig.7,8,9 that the Struve function correctly gives the height of the maxima in $\theta(v)$, with the difference between those two functions being mostly a phase difference that tends to zero as $v \rightarrow \infty$. From the asymptotic form of the Struve function in the limit $v \rightarrow \infty$ we obtain that, in that limit,

$$
\theta(v) \sim \tilde{\omega}_0\frac{\pi}{4}\sqrt{\frac{1}{2\pi v}}\sin(4v - \pi/4) \approx \alpha\,\sin(4v - \pi/4) \quad \text{for} \;\; v \rightarrow \infty.
\tag{30}
$$

where we defined $\alpha \equiv \sqrt{\pi/32}\,\alpha' = \sqrt{\pi/32}\frac{\tilde{\omega}_0}{\sqrt{v}}$, for $v > 1$. We will call α the "DL parameter". Eq. (30) establishes a nice connection between the DL parameter and the amplitude of the oscillations in the function $\theta(v)$.

D. Time-evolution operator

To find out the time evolution of an initial state of the form $|a\rangle$ or $|b\rangle$, we can use the eigenstates at time t=0, as given by Eq.(27). From that equation we can express $|a\rangle$ and $|b\rangle$ in the form

$$
\begin{aligned}
|a\rangle &= \cos\theta|\phi^{-\varepsilon}(0)\rangle \;-\; \sin\theta|\phi^{\varepsilon}(0)\rangle, \\
|b\rangle &= \sin\theta|\phi^{-\varepsilon}(0)\rangle \;+\; \cos\theta|\phi^{\varepsilon}(0)\rangle.
\end{aligned}
\tag{31}
$$

From these, it is now straight forward to construct two orthogonal solutions to Schrödinger's equation which, at $t = 0$, correspond to each one of the eigenstates of H_0 :

$$
|a(t)\rangle = e^{i\varepsilon t}\cos\theta|\phi^{-\varepsilon}(t)\rangle - e^{-i\varepsilon t}\sin\theta|\phi^{\varepsilon}(t)\rangle
$$

and

$$
|b(t)\rangle = e^{i\varepsilon t}\sin\theta|\phi^{-\varepsilon}(t)\rangle + e^{-i\varepsilon t}\cos\theta|\phi^{\varepsilon}(t)\rangle,
\tag{32}
$$

where $|a(0)\rangle = |a\rangle$ and $|b(0)\rangle = |b\rangle$. Using Eq.(24) into above expressions we get

$$
|a(t)\rangle = [\cos\theta K(t)e^{i\varepsilon t} + \sin\theta Z^*(t)e^{-i\varepsilon t}]|a\rangle + [\cos\theta Z(t)e^{i\varepsilon t} - \sin\theta K^*(t)e^{-i\varepsilon t}]|b\rangle
$$

and

$$|b(t)\rangle = [\sin\theta K(t)e^{i\varepsilon t} - \cos\theta Z^*(t)e^{-i\varepsilon t}]|a\rangle + [\sin\theta Z(t)e^{i\varepsilon t} + \cos\theta K^*(t)e^{-i\varepsilon t}]|b\rangle. \tag{33}$$

The time-evolution operator for this system, which is defined by the equation $|\Psi(t)\rangle = U(t,0)\|\Psi(0)\rangle$, can be extracted, in the basis $\{|a\rangle, |b\rangle\}$, directly from the expressions above

$$U_{ab}(t,0) = \begin{bmatrix} u_{aa}(t) & -u_{ba}^*(t) \\ u_{ba}(t) & u_{aa}^*(t) \end{bmatrix}, \tag{34}$$

where,

$$u_{aa}(t) = \cos\theta K(t)e^{i\varepsilon t} + \sin\theta Z^*(t)e^{-i\varepsilon t},$$

$$u_{ba}(t) = \cos\theta Z(t)e^{i\varepsilon t} - \sin\theta K^*(t)e^{-i\varepsilon t}. \tag{35}$$

The subindex ab in U_{ab} is there to remind us of the basis used to represent the time-evolution operator.

Another way to arrive at the same result is by making use of the general expression [Eq.(27) in Milfeld and Wyatt[40]]

$$U(t,0) = \Phi(t)e^{-i\Lambda t}\Phi^{-1}(0) \tag{36}$$

where the columns of the Floquet matrix $\Phi(t)$ are the components of the FES of the system, and Λ is a diagonal matrix whose components are the quasi-energies of the system. For our system, from Eq.(24), the Floquet matrix is

$$\Phi(t) = \begin{bmatrix} K(t) & -Z^*(t) \\ Z(t) & K^*(t) \end{bmatrix}, \tag{37}$$

and $\Lambda = -\varepsilon\sigma_z$.

IV. DYNAMIC LOCALIZATION

It is of particular interest to study the situation where the the system's initial state is a superposition of the eigenstates of H_0. In particular, specially in the context of quantum wells, a particularly interesting initial state is one in which the electron is localized in one of the wells. Such an initial state corresponds to $|\Psi(0)\rangle = |1\rangle \equiv \frac{1}{\sqrt{2}}(|a\rangle + |b\rangle)$, or $|\Psi(0)\rangle = |2\rangle \equiv \frac{1}{\sqrt{2}}(|a\rangle - |b\rangle)$. In this case, we are interested in calculating the probability to find the system at that same location after a time t. The solution can be found by applying the transformation $V = \frac{1}{\sqrt{2}}(\sigma_z + \sigma_x)$, which corresponds to the change of basis $\{|a\rangle, |b\rangle\} \rightarrow \{|1\rangle, |2\rangle\}$, to the evolution matrix in Eq.(34). The resulting matrix, $U_{12} = V U_{ab} V^{-1}$, can be written as

$$U_{12}(t,0) = \begin{bmatrix} u_{11}(t) & -u_{21}^*(t) \\ u_{21}(t) & u_{11}^*(t) \end{bmatrix}, \tag{38}$$

with

$$u_{11} = Re(u_{aa}) + iIm(u_{ba}),$$

$$u_{21} = Re(u_{ba}) - iIm(u_{aa}). \tag{39}$$

It is a well-known fact that dynamic localization occurs only at the points where the quasi-energies vanish, i.e. $\varepsilon(v) = 0$. At this particular values of driving field amplitude v, as it can be seen from Eqs.(34) and (35), the dynamics of the system becomes strictly periodic, with period $2\pi/\omega$, for any initial condition. The points where $\sin\theta(v) = 0$ also produce a periodic evolution of the system (except for an overall time-dependent phase factor), but only for the particular initial conditions $|\Psi(0)\rangle = |a\rangle$ or $|\Psi(0)\rangle = |b\rangle$.

To study the system at the DL points, we will look at the quantity $|u_{11}(t)|^2$, which gives the probability (as a function of time), that the system, if localized in a well (e.g. $|1\rangle$) at time $t = 0$, would remain in that well at a later time t. For $\varepsilon(v) = 0$, and from Eqs.(35,39) we get

$$u_{1,1}(t) = \cos\theta[Re(K(t)) + iIm(Z(t))] + \sin\theta[Re(Z(t)) + iIm(K(t))], \qquad \text{at DL points.} \tag{40}$$

Since this probability is periodic, $u_{1,1}(0) = u_{1,1}(2\pi/\omega) = 1$, it is interesting to see what is the value of this function half-way through a cycle of the field, that is, for $\omega t = \pi$. From Eq.(60) we can deduce that $K(\pi/\omega) = K(0) = \cos\theta$, and $Z(\pi/\omega) = -Z(0) = -\sin\theta$. Using this, we get from the above equation

$$u_{1,1}(\pi/\omega) = \cos\theta^2 - \sin\theta^2 = \cos(2\theta) , \quad \text{at DL points.} \tag{41}$$

We will show in the following figures that the function $\cos(2\theta)$ plays an important role in quantifying how good is the localization of the system at the DL points.

In the lower panels of Figs.7,8,9, we have placed dots on the quasi-energy functions $\varepsilon(v)$, at different values of v. In the upper panel in Figs. 10,11,12 we show, for each one of those points, the corresponding probability $|u_{1,1}(t)|^2$, as given by Eqs. (35),(39). This probability gives the location of the particle, as a function of time, when starting from the initial state $|1\rangle$. In Fig.10 we study the case $\tilde{\omega}_0 = 0.5$. In this plot one can see that the probability evolves in a manner that is typical of the high frequency regime which has been amply studied in the literature. The function can be described as of the form $cos(\varepsilon t)+$ small time-periodic oscillations. Clearly, at the DL points (A,B,C,D), when $\varepsilon = 0$, the probability is exactly periodic (period $2\pi\omega$) and oscillates between 1 and a value that depends on the driving field amplitude v and on $\tilde{\omega}_0$. As derived before, in the middle of the driving period, the probability $|u_{1,1}|^2 = \cos^2(2\theta(v))$.

Given the correspondence between the maxima of $\theta(v)$ and the zeros of $\varepsilon(v)$, we can conclude that the minima of the function $\cos^2(2\theta(v))$ tells us the value of the probability $|u_{1,1}(t)|^2$ half way through the driving field period ($t = \pi/\omega$), at the corresponding DL point (with the exception of point A). This value of $|u_{1,1}(t)|^2$ is very important because it gives us information about the extend to which the particle is localized when the DL points are reached. As we can see in the lower panels of Figs. 10,11,12, when the function $|u_{1,1}(t)|^2$ has a local minimum at $t = \pi/\omega$, then $\cos^2(2\theta(v))$ is close to be the absolute minimum value that $|u_{1,1}(t)|^2$ reaches through out a whole period, $P_l = min(|u_{1,1}|^2)$. It is therefore an important number for describing the amount of localization that can be achieved in the system. When the function $|u_{1,1}(t)|^2$ has a local maximum at $t = \pi/\omega$, then $\cos^2(2\theta(v))$ is still equal to that value but this is not necessarily close to P_l (specially when we are far from the DL regime). This is the case at points B and D in those figures. Surprisingly, however, P_l, for cases B and D, is given, to a certain approximation, by the value of the function $\cos^2(2\theta(v))$ at the minima that corresponds to the *next* DL point. We do not know why this should be so but it was found to be the case in all the cases that we examined. According to this, the DL points can be grouped in pairs, with (B,C) having a similar amount of localization, given by $\cos^2(2\theta(v_c))$; points (D,E) with a localization given by $\cos^2(2\theta(v_E))$, and so on. It is therefore the deeper minima in $\cos^2(2\theta(v))$ that give us directly the amount of localization in the system.

An interesting question to ask, because of practical applications, is whether there is a simple relationship between the amount of localization P_l, $\tilde{\omega}_0$ and v. In other words, given a particular amount of localization P_l, and a given $\tilde{\omega}_0$, what is the required driving field amplitude for the system to achieve such level of localization? To answer this question in the DL regime (were we expect a high level of localization, $P_l \lesssim 1$), one can use Eq.(30) to derive an approximate relationship between P_l, $\tilde{\omega}_0$ and v. At the maxima of $\theta(v)$ (Dl points), $\theta(v) \sim \alpha$, which gives $P_l = \cos(2\theta) \approx 1 - 4\theta^2 = 1 - \frac{\pi}{8}\frac{\tilde{\omega}_0^2}{v}$, from which one finally gets

$$v \approx \frac{\pi\tilde{\omega}_0^2}{8(1 - P_l)}. \tag{42}$$

This simple equation, which has been derived assuming $v > 1$, $\alpha << 1$, already gives good results even for a localization as low as $P_l = 0.5$, with the accuracy improving further for higher values of P_l. For $P_l = 0.5$ the result is $v \sim 0.78\,\tilde{\omega}_0^2$, for $P_l = 0.9$ one obtains $v \sim 4\,\tilde{\omega}_0^2$ and for $P_l = 0.99$ it gives $v \sim 40\,\tilde{\omega}_0^2$.

V. HIGH-ORDER HARMONIC GENERATION

The expected value of the dipole moment of the system can be calculated from the expression

$$\langle d(t)\rangle = \langle\Psi(t)|X|\Psi(t)\rangle = \mu\langle\Psi(0)|\sigma_x(t)|\Psi(0)\rangle , \tag{43}$$

where

$$\sigma_x(t) \equiv U_{ab}(t)^\dagger \sigma_x U_{ab}(t), \tag{44}$$

and using Eqs.(34), we get

$$\sigma_x(t) = \begin{bmatrix} Re[u_{aa}^*(t)u_{ba}(t)] & [u_{aa}^2(t) - u_{ba}^2(t)]^* \\ u_{aa}^2(t) - u_{ba}^2(t) & -Re[u_{aa}^*(t)u_{ba}(t)]. \end{bmatrix}. \tag{45}$$

For a general initial condition of the form $|\Psi(0)\rangle = c_a|a\rangle + c_b|b\rangle$ we get

$$\langle d(t)\rangle/\mu = Re[u_{aa}^*(t)u_{ba}(t)](|c_a|^2 - |c_b|^2) + 2Re[c_a c_b^*(u_{aa}^2(t) - u_{ba}^2(t))]. \tag{46}$$

If we now define the following time-periodic functions,

$$\begin{aligned}
R(t) &\equiv Re(K(t))Re(Z(t)) + Im(K(t))Im(Z(t)) &&\text{(odd harmonics)}, \\
Q(t) &\equiv Re(K(t))Im(K(t)) - Re(Z(t))Im(Z(t)) &&\text{(even harmonics)}, \\
P(t) &\equiv Im(K(t))^2 + Re(Z(t))^2 &&\text{(even harmonics)},
\end{aligned} \tag{47}$$

then, using this, and plugging Eqs.(35) into Eq.(46), we obtain (after some lengthy algebra) the final expression

$$\begin{aligned}
\langle d(t)\rangle/\mu = &[-\sin(2\theta)\cos(2\epsilon t) + 2\cos(2\theta)R(t) + 2\sin(2\theta)\sin(2\epsilon t)Q(t) + 2\sin(2\theta)\cos(2\epsilon t)P(t)]\left(|c_a|^2 - |c_b|^2\right) \\
&+ [\cos(2\theta)\cos(2\epsilon t) + 2\sin(2\theta)R(t) - 2\cos(2\theta)\sin(2\epsilon t)Q(t) - 2\cos(2\theta)\cos(2\epsilon t)P(t)]\,Re(2c_a c_b^*) \\
&+ [-\sin(2\epsilon t) - 2\cos(2\epsilon t)Q(t) + 2\sin(2\epsilon t)P(t)]\,Im(2c_a c_b^*)\ .
\end{aligned} \tag{48}$$

The quantities θ, ε, $P(t)$, $Q(t)$, $R(t)$ depend on v, even though, we do not explicitly indicate so in this notation. We will refer to the initial condition where $|c_a| = 1$ or $|c_b| = 1$ (and therefore $c_a c_b^* = 0$), as the "Optical" Initial Condition (OIC); the case $c_a = \pm c_b$ as the "Tunneling" initial condition (TIC) and the case $c_a = \pm i c_b$ as the "Complex Tunneling" Initial Condition (CTIN).

From the expectation value of the dipole moment, one can obtain the (coherent) emissions spectrum of the system from the expression $|d(\Omega)|^2 = \left|\frac{1}{T}\int_{t_0}^{t_0+T} dt e^{i\Omega t}\langle d(t)\rangle\right|^2$.

Eq.(48) deserves many comments. Notice that generally, there is low-frequency generation, with frequency 2ε for all initial conditions. Only at some particular driving amplitudes this can be prevented. For OIC the low-frequency component can be suppressed only when $\sin(2\theta) = 0$; for TIC only when $\cos(2\theta) = 0$. There is always low-frequency generation at any driving amplitude for CTIC. There is odd-harmonics generation, at frequencies $(2n-1)\omega$ and due to the terms with $R(t)$. This harmonics are generated except when $\cos(2\theta) = 0$ for OIC and except when $\sin(2\theta) = 0$ for TIC. Interestingly enough, CTIN *can not generate odd harmonics*. Even harmonics, at frequencies $2n\omega \pm 2\varepsilon$ occur because of the presence of terms $(\sin(2\epsilon t)$ or $\cos(2\epsilon t))Q(t)$ and $(\sin(2\epsilon t)$ or $\cos(2\epsilon t))P(t)$, and are generated except when $\sin 2\theta(v) = 0$ for OIC and except when $\cos 2\theta(v) = 0$ for TIC. They are always present for *CTIC*.

For a general driven Hamiltonian that possesses the Dynamical Symmetry (DS) $H(x,t) = H(-x, t + \tau/2)$ it has been proven[41] that the HHG from a Floquet eigenstate consists of only *odd*-harmonics. Our Hamiltonian, Eq. (14), is certainly of this kind since the quantum operator that corresponds to x is σ_x, and therefore, if $\sigma_x \to -\sigma_x$, and $t \to t + \tau/2$, the Hamiltonian in Eq. (14) remains the same. According to this, a good check for our result can be done by replacing in Eq.(48) the initial condition $c_a = \cos\theta$, $c_b = \sin\theta$ which corresponds to the initial state being already a Floquet eigenstate [see Eq.(27)]. After doing that, one obtains $\langle d(t)\rangle/\mu = 2R(t)$, which means that this state only generates odd-harmonics, in agreement with the dynamical symmetry arguments developed in the citation above.

As our result (48) shows, in a two-level system it is possible to generate both even *and* odd harmonics. This has also been found in numerical calculations for a double quantum well[42]. The kind of harmonics present in the spectrum is dependent on the initial condition, the driving amplitude and also the phase of the driving field. In this work we have chosen a driving force of the form $\cos(\omega t)$; however, in the most general case of time dependence of the form $\cos(\omega t + \phi)$, the driving phase ϕ, in general, plays an important role in determining the harmonic content of the spectrum. For the case $\sin(\omega t)$ see Gauthey et al[36].

It has been argued[41] that in systems that get ionized during the course of the interaction with the field, only one resonant Floquet state (the one with the longest life-time) contributes to the harmonic spectrum and therefore this could explain the absence of even-harmonic generation in most experiments. There are several experimental results that involve lasers interacting with solid targets, in which even-harmonics and odd harmonics are generated. Even though ionization takes place, the presence of even harmonics has been attributed to the lack of DS in the Hamiltonian. For systems where the main source of harmonic radiation are bound-bound transitions, it is not clear how to justify the use of only one of the FES in the calculation of the HG of the system. In those kinds of system we will argue in future work that, if the evolution of the system is adiabatic under the effect of a laser pulse, then again, only odd-harmonics are generated. For non-adiabatic evolution, we expect to see generation of even and odd harmonics and also dependence on the initial phase of the driving. It is interesting to check our results for the time dependent dipole moment of the system in the DL regime. As we showed before, in the limit of perfect DL, where $v \to \infty$ or $\tilde{\omega}_0 \to 0$, one gets $\theta = 0$, $K(t)$ becomes pure real, $Z(t)$ becomes pure imaginary, and therefore $R(t) = Q(t) = P(t) = 0$. The result for the dipole moment is therefore

$$\langle d(t)\rangle/\mu = \cos(2\epsilon t)Re(2c_a c_b^*) - \sin(2\epsilon t)Im(2c_a c_b^*) = 2|c_a c_b|\cos(2\varepsilon t + \gamma), \tag{49}$$

with γ being the phase difference between c_a and c_b. This is the zeroth-order expression in the first-order perturbative results obtained by Delgado and Gomez-Llorente[23]. Clearly, in this limit there is *no* HG. From this it is clear that in the case of a driven two-level system, DL and HHG are at odds; the greater the localization, the smaller the HHG. The amplitude of any harmonic component of the emission spectrum of the system (except the low frequency one), as a function of increasing driving field strength v should initially increase, then plateau (with oscillations) and finally decrease as v is further increased.

Near the DL regime we can obtain some expressions and compare them with the perturbative results obtained in other works[16,21,23]. For $v > 1$ and $\alpha = \sqrt{\frac{\pi}{32}}\frac{\tilde{\omega}_0}{\sqrt{v}}$, we found that the behavior of the functions $K(t)$ and $Z(t)$ is

$$
\begin{aligned}
K(t) &\approx Re(K(t)) + i\alpha\kappa(t) \\
Z(t) &\approx \alpha\zeta(t) + iIm(Z(t)).
\end{aligned}
\tag{50}
$$

Here $\kappa(t)$ and $\zeta(t)$ are periodic functions (even and odd respectively) with amplitude close to one. As we have shown before, in this regime, the amplitude of the oscillations in the function $\theta(v)$ is also proportional to α. According to this, and using Eq.(47), we see that in this regime, $R(t) \propto \alpha$, $Q(t) \propto \alpha$, $P(t) \propto \alpha^2$. We now rewrite Eq.(48) in a form that makes evident the magnitude of the different terms that contribute to the dipole moment,

$$
\begin{aligned}
\langle d(t)\rangle \approx & \left[-\alpha\tilde{\theta}\cos(2\epsilon t) + \alpha\tilde{R}(t) + 2\alpha^2\tilde{\theta}\sin(2\epsilon t)\tilde{Q}(t) + 2\alpha^3\tilde{\theta}\cos(2\epsilon t)\tilde{P}(t)\right]\left(|c_a|^2 - |c_b|^2\right) \\
& + \left[\cos(2\epsilon t) - 2\alpha\sin(2\epsilon t)\tilde{Q}(t) + 4\alpha^2\tilde{\theta}\tilde{R}(t) - 2\alpha^2\cos(2\epsilon t)\tilde{P}(t)\right]Re(2c_a c_b^*) \\
& + \left[-\sin(2\epsilon t) - 2\alpha\cos(2\epsilon t)\tilde{Q}(t) + 2\alpha^2\sin(2\epsilon t)\tilde{P}(t)\right]Im(2c_a c_b^*)\ .
\end{aligned}
\tag{51}
$$

where $\tilde{R}(t) = R(t)/\alpha$, $\tilde{Q}(t) = Q(t)/\alpha$, $\tilde{P}(t) = P(t)/\alpha^2$, and $\tilde{\theta} = \theta/\alpha \sim \sin(4v - \pi/4)$. From this expression we can see that in the DL regime, OIC generates low frequency and odd-harmonic radiation to second order in α and even harmonic generation is forth order in this parameter. For TIC there is strong low frequency generation independent of any of the parameters of the system (provided we are in DL regime); even harmonic generation is second order and odd harmonic generation is forth order in α. For CTIC the situation is similar to TIC except that no odd-harmonic radiation is generated at all.

As mentioned before, from the general expression for the dipole moment, since $\varepsilon = \varepsilon(v)$ and $\theta = \theta(v)$, with successive points where either $\theta(v)$ or $\varepsilon(v)$ vanish, there is a lot of variation in the composition (in terms of odd or even harmonics) of the spectrum of this system as a function of the amplitude of the driving field. The interesting exception being the CTIC where even harmonics are always generated and odd harmonics are never generated.

In Fig.13, 14 and 15 we show the emission spectrum for three distinct initial conditions (OIC,TIC,CTIC) and for two values of the driving field amplitude. What is common to all this plots is the typical profile of harmonic generation that has been found theoretically and experimentally in different systems. It consists of a plateau where the amplitudes are of similar magnitude (fluctuations are of one to two orders of magnitude typically), followed by a frequency cut-off after which the harmonic amplitudes decay very quickly (exponentially in $n\omega$).

From the structure of the FES, like the one shown in Fig. 6, one can see that there is a cut-off in the harmonic components of the eigenstates, which occurs at $N_e = 2v - 1$ (for $v \geq 1$). The location of the cut-off in the emission spectrum of the system follows from the location of the cut-off in the eigenstates, since the functions $R(t), Q(t), P(t)$ are second order in the FES components. $R(t), Q(t), P(t)$ therefore have cut-offs at $N_{cut} = 2N_e = 4v - 2$. This is the same cut-off that we expect to see in the emission spectrum of the system.

As we can see in Fig. 13, 14, 15, this result describes quite well the location of the last peak before the components start to decay exponentially. The linear dependence of N_{cut} on the amplitude of the field implies that $N_{cut} \propto \sqrt{I}$, where I is the intensity of the field. This result is expected for HHG in systems where bound-bound transitions are dominant[46,47]. For dominant bound-continuum transitions[48], $N_{cut} \propto I$.

In Fig.13 we show the emission spectrum for OIC, and for two different values of the driving amplitude. For $v = 4.15$ (which gives $\theta \approx 0$), we see, from the first line of Eq.(51)that one expects no low frequency component, odd harmonics and no even harmonics. For $v = 4.5$ (which gives $\varepsilon \approx 0$), we obtain a strong low frequency component, strong odd-harmonic components and very weak even-harmonics components that are due to the function $P(t)$ only (since at $\varepsilon = 0$, $\sin(2\epsilon t) = 0$ and therefore $Q(t)$ does not contribute to the spectrum). This is a special case since in general, in this regime, $Q(t)$'s contribution to $|d(\Omega)|^2$ is two orders of magnitude bigger than the one from $P(t)$.

In Fig. 14 we show the emissions spectrum for TIC for the same values of v as before. In the $\theta = 0$ case, we can see, from the second line in Eq.(51), that there is a strong low frequency component ($\Omega = \pm 2\varepsilon$), no odd-harmonics and split even harmonics ($\Omega = 2n \pm 2\varepsilon$). For the case $\varepsilon = 0$ there is a zero frequency component and also odd and even harmonics (not split) of the same magnitude.

Finally, in Fig. 15 we show the case when the initial condition is CTIC. From the third line in Eq.(51) we see that, for the case $\theta = 0$ we should get a strong low frequency component and split even harmonics. For $\varepsilon = 0$ case there is no static component, only even harmonics (not split).

For the characteristic plateau of HHG to appear, it was shown[28] that $v \geq \sqrt{\tilde{\omega}_0}$. In this region we have found numerically that $\cos(2\theta) \neq 0$, which means that in the OIC, overall, the odd harmonics are much more stable with respect to changes in the driving amplitude that the even harmonics, which as a whole, do fluctuate with v (following the behavior of $\sin(2\theta)$). As one approaches the DL regime the odd harmonics will dominate the spectrum for the OIC (which is the initial condition most easily obtained experimentally). It is easy to derive an estimate for the conditions under which odd-harmonics will dominate over even harmonics in the OIC. For that we take $\alpha \geq 0.1$, so that there is at least one order of magnitude difference in their contributions to Eq.(49). From $\alpha = \sqrt{\frac{\pi}{32}} \frac{\tilde{\omega}_0}{\sqrt{v}}$ one gets the estimate

$$v \gtrsim 10\tilde{\omega}_0^2.$$

When this condition is satisfied, odd harmonics will clearly dominate the spectrum in the OIC.

VI.   SUMMARY AND CONCLUSIONS

In this work we used a complete Floquet-Green operator formalism for the analytical solution of a harmonically driven two level system. From this operator we were able to completely solve the system and obtain the quasi-energies and the eigenstates in terms of continued fractions.

We found that the oscillatory behavior of the quasi-energies of the system can be interpreted as due to multi-photon resonances that occur in an increasingly periodic way as the strength of the driving field is increased. This multi-photon resonances involve an odd number of photons and produce avoided crossings centered at the edges of the energy Brillouin zone $\varepsilon = \pm 0.5$. The width and amplitude of them increases with the driving field amplitude. The structure of the continued fractions from which the quasi-energies can be obtained made it clear that this is the case, since each term in the continued fraction was found to be related to the inclusion of a particular basis state in the calculations, and each avoided crossing studied did only appear when the corresponding term in the continued fraction was included.

We were able to obtain analytical expressions for the components of the Floquet eigenstates and from them we constructed the time-evolution operator of this system. The structure of the eigenstates revealed a characteristic pattern, with a "chaotic" region where the components are sensitive to small changes in v, change sign and have zeros, and a "regular" region where the components depend less sensitively on v, and decay exponentially with the frequency $n\omega$. The cut-off frequency that divides the two regions and gives the position of the largest floquet component of the eigenstates is proportional to the driving field strength v, $N_e = 2v - 1$, a result that is valid for any $\tilde{\omega}_0$ (provided $v > \sqrt{\tilde{\omega}_0}$).

From the time evolution operator we were able to study the Dynamic Localization phenomena which is one of the important features of this Hamiltonian. It is known that DL is obtained at values of the driving field strength for which the quasi-energies vanish. In Quantum Computation, this localization mechanism can be of great importance for controlling the state of a q-bit (as realized for example in a solid state devise such as a double quantum well or a Josephson Junction), since the amount of tunneling of an electron between two adjacent wells can be varied with the intensity of the driving field. In this work we obtained a correlation between the DL points and the maxima of the quantity $\theta(v)$ that describes the Floquet eigenstates of the system. Also, the value of the function $\cos^2(2\theta(v))$, at its lowest minima, was found to give a good approximation to the degree of localization of the system at the corresponding DL points. These points appear in pairs with simmilar degrees of localization corresponding to each pair. We also found the equation

$$v \approx \frac{\pi\tilde{\omega}_0^2}{8(1 - P_l)},$$

which, at the DL points, relates the degree of localization P_l, with the energy level difference ω_0, and the amplitude v of the driving field (all quantities in units of $\hbar\omega$). This equation can be used to easily estimate the amount of localization achievable in this system for a given set of parameters.

For the study of High Harmonic Generation in this system we calculated the expected value of the dipole moment which revealed that the emission spectrum, in general, can contain a low frequency component and odd and even harmonics. The particular components and their amplitudes depend strongly on the initial state of the system and on the specific driving field amplitude. We found that there exists an initial condition (Complex Tunneling) of the driven two-level system for which no odd-harmonics can be generated at any driving field strength. For each one of the "pure" initial conditions, namely Optical (OIC), Tunneling (TIC) or Complex Tunneling (CTIC), the driving

amplitudes where the $\theta(v) = 0$ produce either pure even harmonic generation or pure odd harmonic generation, depending on the particular initial condition. For all other driving amplitudes there will be in general generation of both kinds of harmonics (except for CT initial condition). When the initial state is a Floquet eigenstate, we found that only odd-harmonics are generated, a result that is expected from the Dynamical Symmetry (DS) of the Hamiltonian. In general we can say that the emission spectrum of the driven two-level system is sensitive to different parameters, such as the initial preparation, the amplitude of the driving and its phase (phase dependence will be explored in future work).

For small values of α, but still not deep into the DL regime ($\alpha \approx 0.15$) we showed the different magnitude of the terms that give low frequency, even harmonics and odd harmonics. In the Optical Initial Condition (OIC) we found that odd harmonic generation is stronger, with even harmonics weaker and even nonexistent for particular values of the driving field amplitude (when $\theta(v) = 0$). For Tunneling Initial Condition (TIC), even harmonics dominate, except at the DL points ($\varepsilon = 0$), where even and odd harmonics have approximately the same amplitude. For Complex Tunneling Initial Condition (CTIC) no odd harmonics are generated.

Well inside the DL regime, odd harmonics are almost exclusively generated in the Optical Initial Condition, and even harmonics in both of the Tunneling Initial Conditions. In this regime of high localization, Harmonic generation decreases with decreasing α, a situation that clearly places both effects on opposite sides of the parameter space, although with significant overlap between them. In general, for a driven two level system, the strongest HHG should occur for higher values of $\tilde{\omega}_0$ and for driving amplitudes $v \lesssim 10\tilde{\omega}_0^2$ (for $\alpha > 0.1$). For strong DL, smaller values of $\tilde{\omega}_0$ and/or bigger values of v are required, $v \gtrsim 10\tilde{\omega}_0^2$ (for $\alpha < 0.1$). *Strong* HHG in a two-level system is an eminently non-linear, non-perturbative phenomenon.

The driven two-level model has been shown to be useful in understanding the basic features of high-harmonic generation experimentally observed in atoms and molecules, even though obviously the full complexity of the general processes in atoms and molecules can not be accounted for with this model. The model predicts an emission spectrum with a plateau and a cut-off frequency ($N_{cut} = 4v - 2$), whose location depends on the square-root of the intensity of the driving field (since $v \propto E \propto \sqrt{I}$). Such dependence has been found in systems where bound-bound transitions account for most of the HHG[46,49]. For the case of charge-resonant states of odd-charge molecular ions it has also been argued[21] that this simple two-level model can account for the behavior of these molecules in a strong laser pulse. A square-root dependence of the cut-off frequency with the intensity of the laser field can be found in several experiments[45], a fact that is characteristic of a driven two-level system and which might point in the direction of an effective two-level dynamics for some systems[28].

HHG and DL are the two mayor features of a driven two-level system with a great range of applications in atomic and solid state systems where coherent sources of radiation and control of quantum states are sought. Through this work we have established a strong connection between this two phenomena and provided a detailed description and a deeper understanding of this system.

Appendix A: components of the FES

From the definition of the Floquet-Green operator, we have shown in Eq.(10) that the residue of the function $\mathcal{G}_{0,0}(E)$ at a pole $E = \varepsilon + p$ is the operator (2x2 matrix) $|\phi_p^\varepsilon\rangle\langle\phi_p^\varepsilon|$, where $|\phi_p^\varepsilon\rangle$ is the *pth* Fourier component of the Floquet eigenstate corresponding to the quasi-energy ε. If we write $|\phi_p^\varepsilon\rangle \equiv K_p|a\rangle + Z_p|b\rangle$, then, in principle, from the residue (a matrix) of $\mathcal{G}_{0,0}$ we could determine the components K_p, Z_p. This is only true, however, provided the residue does not turn out to be a diagonal matrix. Unfortunately, this is the case for the system we are considering, since, as we mentioned before, $G_{0,0}(E)$ *is* a diagonal matrix ($V_{eff}(E)$ is diagonal) and therefore, its residue only gives us information about $|K_p|^2$ and $|Z_p|^2$. From Eq.(8) we can see that the off-diagonal components $G_{m,0}$ can give us the needed components:

$$\mathcal{G}_{m,0}(E) = \sum_{\gamma,p} \frac{1}{E - \varepsilon_\gamma - p} |\phi_{m+p}^{\varepsilon_\gamma}\rangle\langle\phi_p^{\varepsilon_\gamma}| \ . \tag{52}$$

From this we get that at the pole $E = \varepsilon_\gamma$ (and therefore $p = 0$), the residue is $|\phi_m^{\varepsilon_\gamma}\rangle\langle\phi_0^{\varepsilon_\gamma}|$. From all these residues for all values of m, one could therefore extract all the eigenvector components $|\phi_m^{\varepsilon_\gamma}\rangle$.

The $\mathcal{G}_{m,0}$ operators can be obtained from $\mathcal{G}_{0,0}$, as it was shown in Ref.[26]. The result is

$$
\begin{aligned}
\mathcal{G}_{1,0} &= F_0^+ \mathcal{G}_{0,0} \ , \\
\mathcal{G}_{2,0} &= F_1^+ \mathcal{G}_{1,0} = F_1^+ F_0^+ \mathcal{G}_{0,0} \ , \\
&\ \ \vdots
\end{aligned}
\tag{53}
$$

$$
\mathcal{G}_{m,0} = F_{m-1}^+ \mathcal{G}_{m-1,0} = \prod_{j=0}^{m-1} F_j^+ \mathcal{G}_{0,0}(E) \ , \qquad \text{for m} > 0,
$$

and where (showing explicitly the energy dependence)

$$
F_j^+(E) \equiv (V\mathcal{F}_{j,0}(E))^{-1}V = V^{-1}V_{\text{eff}}^+(E+j) = \begin{bmatrix} 0 & \frac{1}{v}v_b^+(E+j) \\ \frac{1}{v}v_a^+(E+j) & 0 \end{bmatrix} \ ,
\tag{54}
$$

and similarly,

$$
\mathcal{G}_{-m,0}(E) = \mathcal{F}_{-m+1}^- G_{-m+1,0} = \prod_{j=0}^{m-1} \mathcal{F}_{-j}^- G_{0,0} \qquad \text{for m} > 0,
\tag{55}
$$

with

$$
F_{-j}^-(E) \equiv (V\mathcal{F}_{-j,0}(E))^{-1}V = V^{-1}V_{\text{eff}}^-(E-j) = \begin{bmatrix} 0 & \frac{1}{v}v_b^-(E-j) \\ \frac{1}{v}v_a^-(E-j) & 0 \end{bmatrix} \ .
\tag{56}
$$

It is not difficult to show using Eqs.(52), (53), and (55), that

$$
|\phi_{m+1}^{\varepsilon_\gamma}\rangle = F_m^+(\varepsilon_\gamma)|\phi_m^{\varepsilon_\gamma}\rangle
$$

and

$$
|\phi_{m-1}^{\varepsilon_\gamma}\rangle = F_m^-(\varepsilon_\gamma)|\phi_m^{\varepsilon_\gamma}\rangle \ ,
\tag{57}
$$

with $\varepsilon_\gamma = \pm\varepsilon$.

As we already mentioned, at $E = \varepsilon$ the residue of $G_{0,0}(E)$ is proportional to $|b\rangle$ and at $E = -\varepsilon$ the residue is proportional to $|a\rangle$. From this, and using Eq.(57) together with Eqs.(54) and (56), we can write explicitly the two Floquet eigenstates of this system:

$$
|\phi^{-\varepsilon}(t)\rangle = N[\dots + \frac{e^{2i\omega t}}{v^2}v_b^-(-\varepsilon - 1)v_a^-(-\varepsilon)|a\rangle \ + \ \frac{e^{i\omega t}}{v}v_a^-(-\varepsilon)|b\rangle \ + \ |a\rangle +
$$

$$
+ \ \frac{e^{-i\omega t}}{v}v_a^+(-\varepsilon)|b\rangle \ + \ \frac{e^{-2i\omega t}}{v^2}v_b^+(-\varepsilon + 1)v_a^+(-\varepsilon)|a\rangle \ + \dots]
$$

and

$$
|\phi^{\varepsilon}(t)\rangle = N[\dots + \frac{e^{2i\omega t}}{v^2}v_a^-(\varepsilon - 1)v_b^-(\varepsilon)|b\rangle \ + \ \frac{e^{i\omega t}}{v}v_b^-(\varepsilon)|a\rangle \ + \ |b\rangle \ +
$$

$$
+ \ \frac{e^{-i\omega t}}{v}v_b^+(\varepsilon)|a\rangle \ + \ \frac{e^{-2i\omega t}}{v^2}v_a^+(\varepsilon + 1)v_b^+(\varepsilon)|b\rangle \ + \dots],
\tag{58}
$$

with N being a normalization constant. If we use the symmetry relations, $v_b^-(-E) = -v_a^+(E)$ and $v_b^+(-E) = -v_a^-(E)$ we can write this two eigenstates in a more compact way,

$$
|\phi^{-\varepsilon}(t)\rangle = K(t)|a\rangle \ + \ Z(t)|b\rangle
$$

and

$$|\phi^{\varepsilon}(t)\rangle = -Z(t)^{*}|a\rangle \; + \; K(t)^{*}|b\rangle \; , \tag{59}$$

with

$$K(t) = N(.... + \frac{e^{4i\omega t}}{v^4}v_b^-(-\varepsilon-3)v_a^-(-\varepsilon-2)v_b^-(-\varepsilon-1)v_a^-(-\varepsilon) \; + \; \frac{e^{2i\omega t}}{v^2}v_b^-(-\varepsilon-1)v_a^-(-\varepsilon)+1$$

$$+ \; \frac{e^{-2i\omega t}}{v^2}v_b^+(-\varepsilon+1)v_a^+(-\varepsilon) \; + \; \frac{e^{-4i\omega t}}{v^4}v_b^+(-\varepsilon+3)v_a^+(-\varepsilon+2)v_b^+(-\varepsilon+1)v_a^+(-\varepsilon))$$

$$= N[\sum_{n=-\infty}^{\infty} e^{-2in\omega t}K_{2n}(-\varepsilon)] \; ,$$

$$Z(t) = N[...\frac{e^{3i\omega t}}{v^3}v_a^-(-\varepsilon-2)v_b^-(\varepsilon-1)v_a^-(-\varepsilon)+ \; \frac{e^{i\omega t}}{v}v_a^-(-\varepsilon)+\frac{e^{-i\omega t}}{v}v_a^+(-\varepsilon) \; + \; \frac{e^{-3i\omega t}}{v^3}v_a^+(-\varepsilon+2)v_b^+(-\varepsilon+1)v_a^+(-\varepsilon)....]$$

$$= N[\sum_{n=-\infty}^{\infty} e^{-i(2n-1)\omega t}Z_{2n-1}(-\varepsilon)]$$

$$\tag{60}$$

where N is a normalization constant so that $|K(t)|^2 + |Z(t)|^2 = 1$, and we have

$$K_{2n}(-\varepsilon) = \begin{cases} 1 & \text{for } n = 0, \\ \prod_{j=1}^{|n|} \frac{1}{v^2}v_b^{sg(n)}(-\varepsilon+sg(n)(2j-1))v_a^{sg(n)}(-\varepsilon+sg(n)(2j-2))) & \text{for } |n| > 0 \end{cases}$$

$$Z_{2n+1}(-\varepsilon) = \begin{cases} \frac{1}{v}v_a^+(-\varepsilon+2n)K_{2n}(-\varepsilon) & \text{for } 2n+1 > 0, \\ \frac{1}{v}v_a^-(-\varepsilon+2n+2)K_{2n+2}(-\varepsilon) & \text{for } 2n+1 < 0, \end{cases}$$

$$\tag{61}$$

and we used $sg(x) \equiv x/|x|$.

---

[1] B.W. Shore, in *The Theory of coherent Atomic Excitation* (Wiley, New York, 1990).
[2] F. Großmann, T. Dittrich, P. Jung, and P. Hänggi, Phys.Rev.Lett. 67, 516 (1991).
[3] M. Holthaus, Phys.Rev.Lett. 69, 351 (1992).
[4] R. Aguado and G. Platero, Phys.Rev. B 55, 12860 (1997).
[5] Y. Dakhnovskii and H. Metiu, Phys. Rev. B 51, 4193 (1995).
[6] R. Aguado, J.Iñarrea, and G. Platero, Phys.Rev. B 53, 10030 (1996).
[7] M. Holthaus, D.W. Hone, Phys.Rev.B 49, 16 605 (1994).
[8] P. Meystre, Opt.Comm. 90, 41 (1992), and refferences therein.
[9] S.H. Autler and C.H. Townes, Phys. Rev. 100, 703 (1955).
[10] J.H. Shirley, Phys. Rev. 138, B 979 (1965).
[11] W.M. Ruyten, Phys. Rev. A 42, 4226 (1990).
[12] S. Stenholm, J. Phys. B: At.Mol.Phys. 5, 878 (1972).
[13] G.S. Agarwal and N. Nayak, J. Phys. B: At.Mol.Phys. 19, 3385 (1986).
[14] X.G. Zhao, Phys. Rev. B 49, 16 753 (1994).
[15] H. Wang, Phys. Lett. A 217, 225 (1996).
[16] Y. Dakhnovskii and R. Bavli, Phys. Rev. B 48, 11020 (1993).
[17] A. Sacchetti, J. Phys. A: Math. Gen. 34, 10293 (2001).
[18] M. Frasca, Phys. Rev. B 68, 165315 (2003).
[19] J.C.A. Barata and W.F. Wreszinski, Phys. Rev. Lett. 84, 2112 (2000).
[20] D.H. Dunlap and V.M. Kenkre, Phys. Rev. B 34, 3625 (1986).
[21] M.Yu. Ivanov and P.B. Corkum, Phys. Rev. A 48, 580 (1993).
[22] A. Santana, J.M. Gomez Llorente and V. Delgado, J. Phys. B: At. Mol. Opt. Phys. 34, 2371 (2001).
[23] V. Delgado and J.M. Gomez Llorente, J. Phys. B: At. Mol. Opt. Phys. 33, 5403 (2000).
[24] H.Sambe, Phys. Rev. A 7, 2203, 1972.
[25] F.H.M Faisal, Comp. Phys. Rep. 9, 55, (1989).
[26] D.F. Martinez, J. Phys. A: Math.Gen. 36, 9827 (2003).
[27] K. Drese and M. Holthaus, Eur. Phys. J. D 5, 119 (1999).
[28] A.E. Kaplan and P.L. Shkolnikov, Phys. Rev. A 49, 1275 (1994).
[29] D. Dimitrovski, E.A. Solov'ev, J.S. Briggs, Phys. Rev. Lett. 93, 083003 (2004).

[30] R. Gush and H.P. Gush, Phys. Rev. A, 6, 129 (1972).

[31] J.M. Villas-Bôas, W. Zhang, S.E. Ulloa, P.H. Rivera, and N. Studart, Phys. Rev. B 66, 085325 (2002).

[32] For the resonant case, we have obtained a numerical fit, that can be used for any value of v. It was obtained by displacing the first couple of zeros of the Bessel function $J_0(4v)$ to the left, and linearizing the initial behavior by multiplying this function by a suitable factor. The resulting expression that approximates the behavior of $\epsilon(v)$ to two decimal points is
$\epsilon(v) \simeq \frac{1}{2}(0.5353 + 1.7(v - 0.5228)^2)\frac{1+(2v)^4}{1+(0.5353+1.7(v-0.5228)^2)(2v)^4} J_0\left(4v + \frac{0.6}{1+5(v-0.5228)^2}v\right)$

[33] Clearly, in the limit $n \to \infty$, $F_n^{\pm}(E) \to F^{\pm}(E)$. Even though the convergence of continued fractions is a complex mathematical subject, we have not yet found a continued fraction related to a physical system which failed to have a limit. For all calculations that involve a C.F. in this paper, convergence to any specified precision was always achieved.

[34] J.G. Eden, Prog. Quantum Electron. 28, 197 (2004).

[35] B. Sundaram and P.W. Milonni, Phys. Rev. A 41, R6571 (1990).

[36] F.I. Gauthey, C.H. Keitel, P.L. Knight and A. Maquet, Phys. Rev. A 52, 525 (1995).

[37] F.I. Gauthey, C.H. Keitel, P.L.Knight and A. Maquet, Phys. Rev. A 55, 615 (1997), F.I. Gauthey, B.M. Garraway and P.L. Knight, Phys. Rev. A 56, 3093 (1997).

[38] M.L. Pons, R. Taïeb and A. Maquet, Phys. Rev. A 54, 3634 (1996).

[39] M. Abramowitz and I.A. Stegun, Handbook of Mathematical Functions (Dover, New York, 1965), p.497.

[40] K.F. Milfeld and R.E. Wyatt, Phys. Rev. A 27, 72 (1983).

[41] N. Ben-Tal, N. Moiseyev and A. Beswick, J.Phys. B:At.Mol. Opt. Phys. 26, 3017 (1993);O.E. Alon, Vitali Averbukh, N. Moiseyev, Phys. Rev. Lett. 80, 3743 (1998).

[42] R. Bavli and H. Metiu, Phys. Rev. A 47, 3299 (1993).

[43] H. Wang, V.N. Freire, and X.G. Zhao, Phys. Rev. A 58, 1531 (1998).

[44] M. Protopapas, C.H. Keitel and P.L. Knight, Rep. Prog. Phys. 60, 389 (1997) and references therein.

[45] (a) A. L'Huillier, K. J. Schafer, and K.C. Kulander, J.Phys. B 24, 3315 (1991);(b) A. L'Huillier, K. J. Schafer, and K.C. Kulander, Phys. Rev. Lett. 66, 2200 (1991); (c) A. L'Huillier, L.-A. Lompré, G. Mainfray and C. Manus, in atoms in intense laser Field, edited by M. Gavrila (academic, boston, 1992), p. 139.

[46] V. Averbukh, O.E. Alon, and N. Moiseyev, Phys. Rev. A 64, 033411 (2001).

[47] P. Žďánská, V. Averbukh, and N. Moiseyev, J. Chem. Phys. 118, 8726 (2003).

[48] P.B. Corkum, Phys. Rev. Lett. 71, 1994 (1993); K.C. Kulander, K.J. Schafer, and J.L. Krause, in Super-Intense Laser-Atom Physics, Vol. 316 of NATO Advanced Study Institute, Series B: Physics, edited by B. Pirax, A. L'Huillier, and K. Rzewski, (Plenum Press, New York, 1993), p. 95; M. Lewenstein, Ph. Balcou, M.Yu. Ivanov, A. L'Huillier, and P.B. Corkum, Phys. Rev. A 49, 2117 (1994).

[49] A.K. Gupta, O.E. Alon, and N. Moiseyev, Phys. Rev. B 68, 205101 (2003).
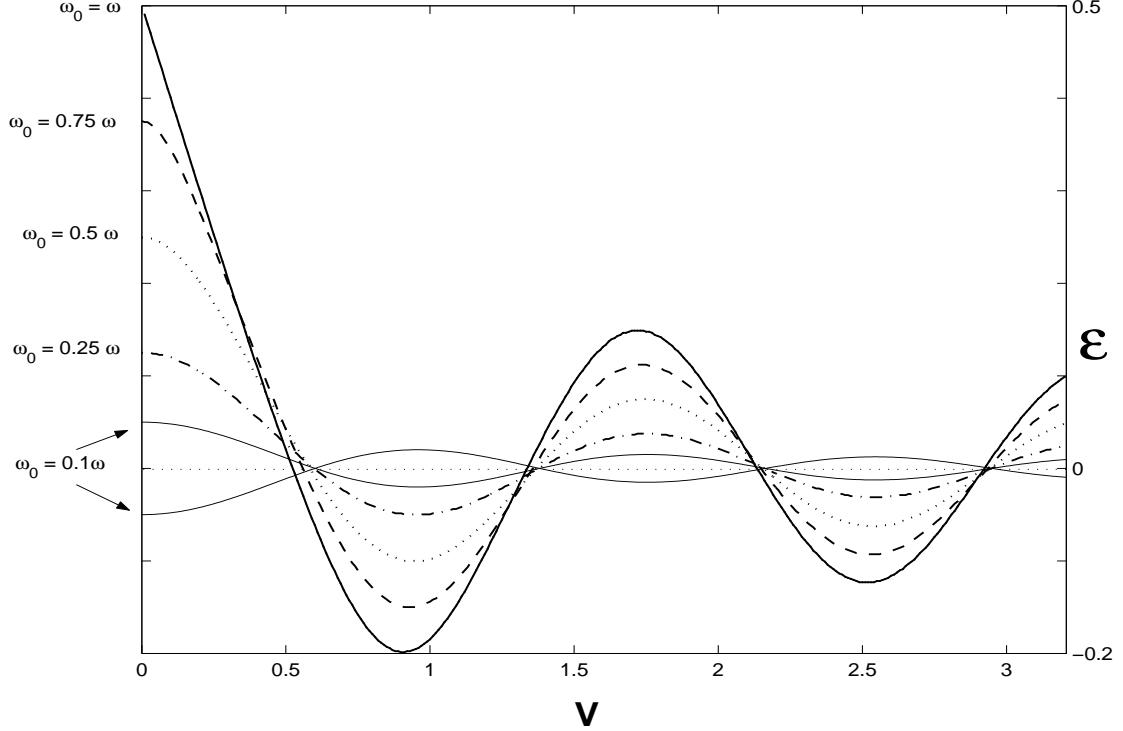
FIG. 1: Quasi-energy as a function of driving amplitude (v), for different values of $\tilde{\omega}_0 \equiv \omega_0/\omega \leq 1$ (high frequencies) .
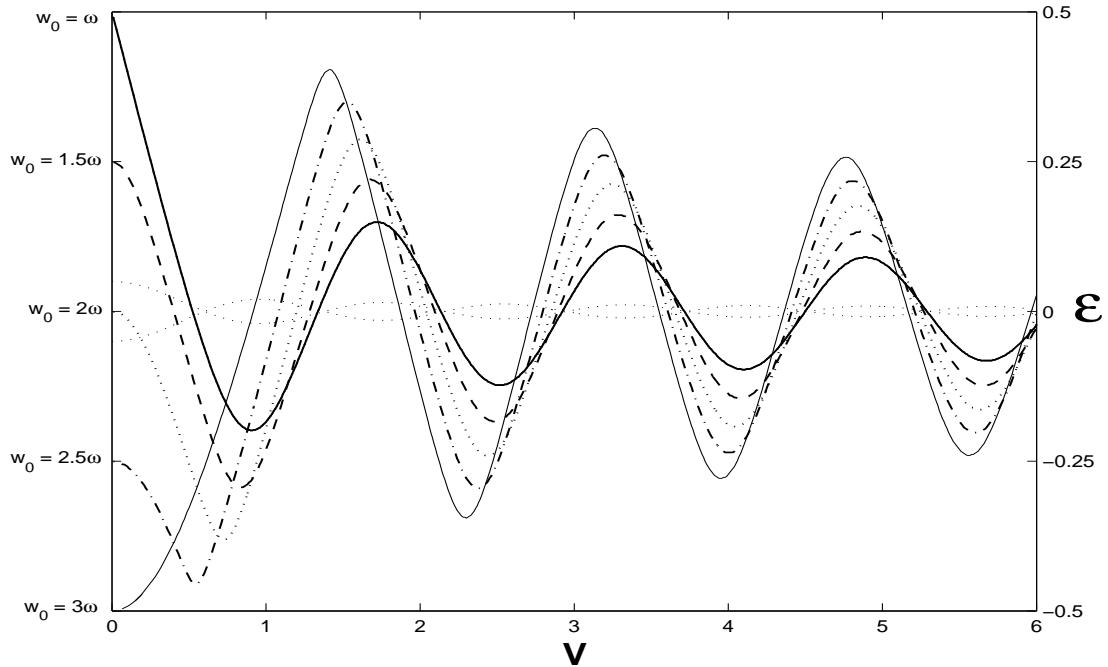

FIG. 2: Quasi-energy as a function of driving amplitude, for different values of $\tilde{\omega}_0 \geq 1$ (low frequencies). The functions $\pm 0.05 J_0(4v)$ are plotted with dotted lines for comparison.
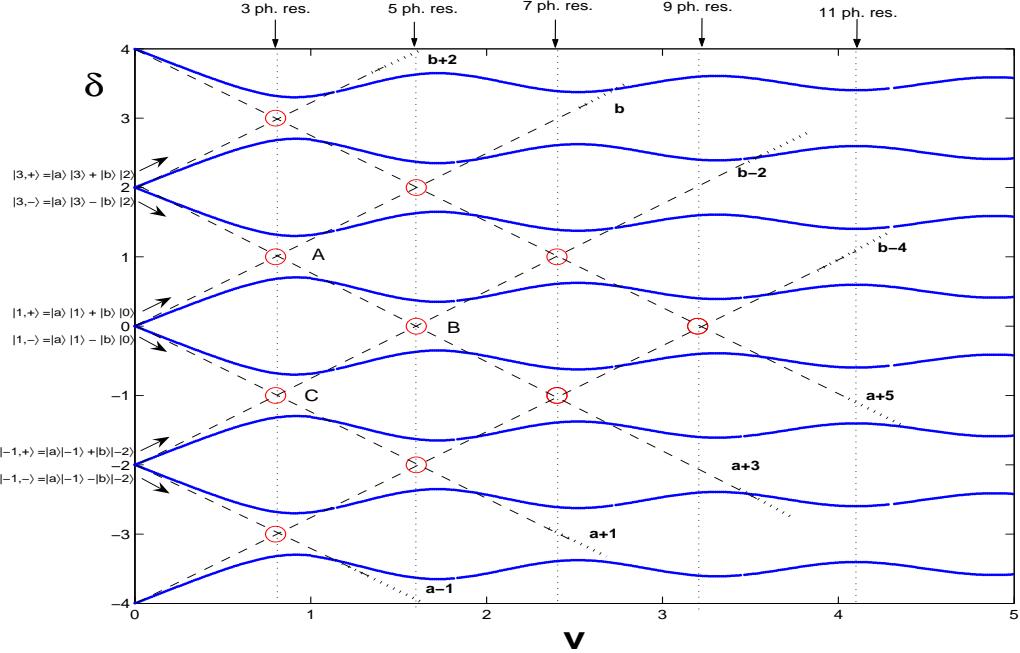
FIG. 3: Solutions of Eq. (20) as a function of driving amplitude for the resonant case ($\tilde{\omega}_0 = 1$). The avoided crossings structure can be accounted for, in an approximate way, by a set of crossings of the eigenvalues corresponding to the first-order FES indicated on the left of the figure. Avoided crossings A and C are mainly due to a 3 photon resonance between the corresponding FES; B corresponds to a 5 photon process.
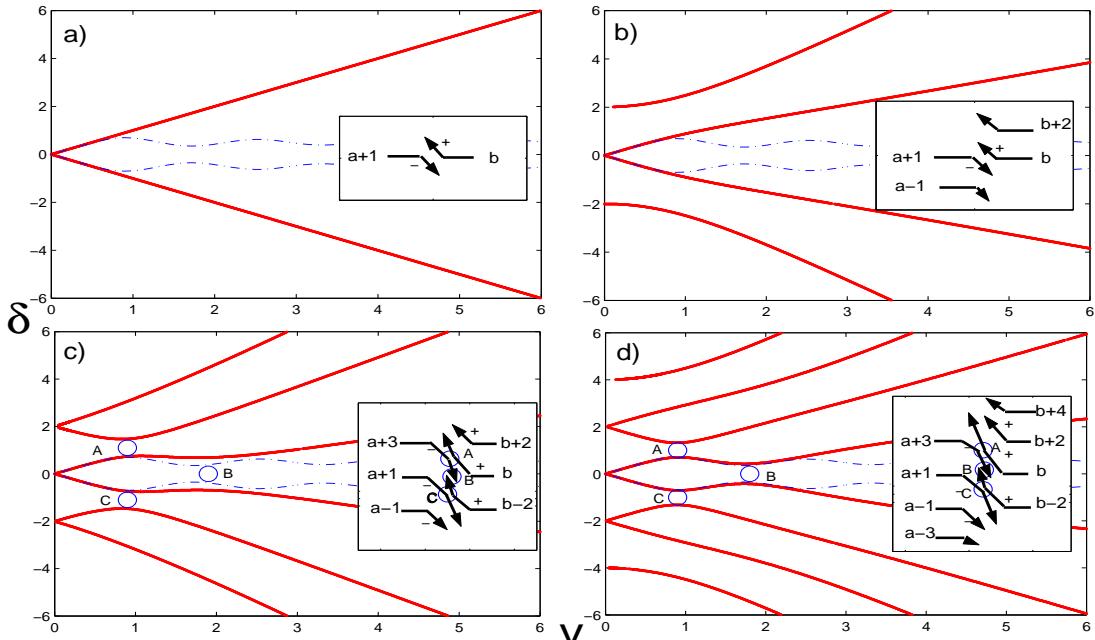
FIG. 4: Solutions of truncated versions of Eq. (22): $F_n^+ F_n^- = v^2$, for different values of n. In a) n=0; b) n=1; c) n=2; d)n=3. The labels $b - 2n$ and $a - 2m - 1$ correspond to terms in the CFs in Eq. (23) of the form $\delta + 2n$ and $\delta + 2m + 1 + \tilde{\omega}_0$. As more terms are included new avoided crossings appear. The $\pm$ signs are used to indicate each one of the two solutions that originate at the points $\delta = 2n$ in the y-axis.
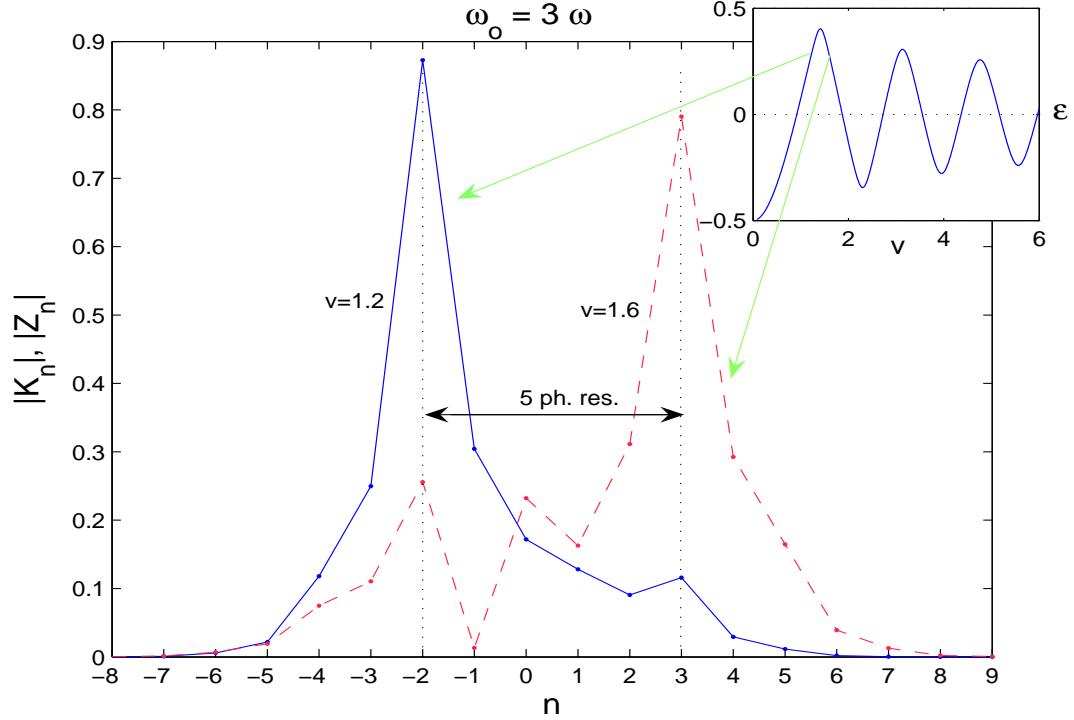
FIG. 5: Components of the FES for $\tilde{\omega}_0 = 3$ and for two diffrent values of the driving amplitude ($v = 1.2,\ 1.6$). The avoided crossing that occurs near $v \sim 1.4$ is due to a 5 photon process between two first-order FES.
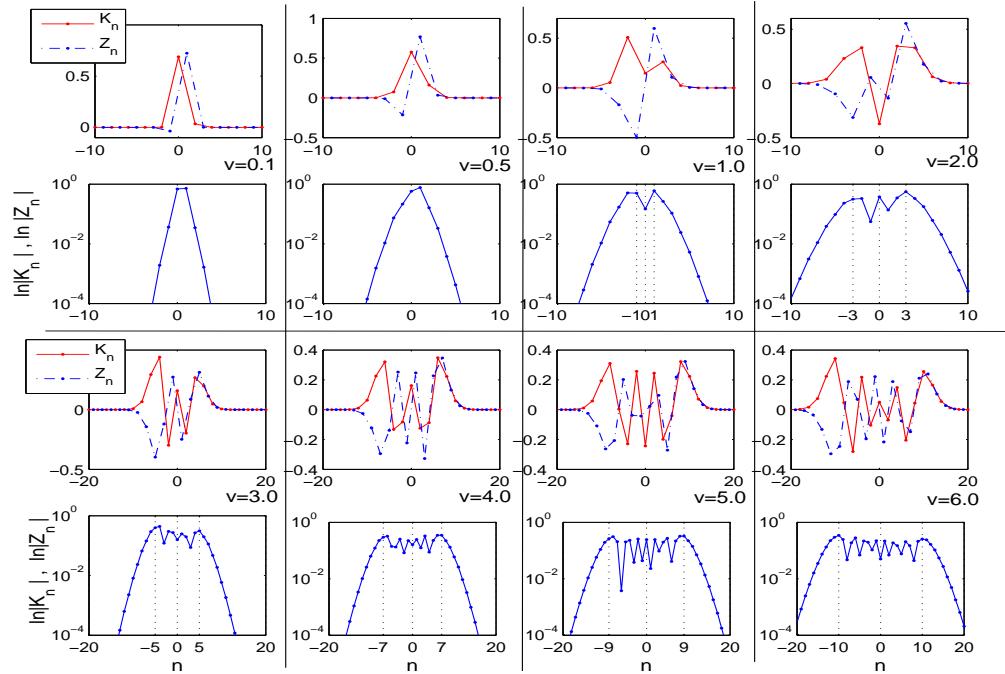
FIG. 6: Components of the FES for $\tilde{\omega}_0 = 1$ and for eight different values of the driving amplitude. The logaritmic plots show the "plateau" structure of the FES, which gives rise to the well-known plateau studied in HHG. The cut-off location (N_e) follows the approximate rule $N_e = 2v - 1$.
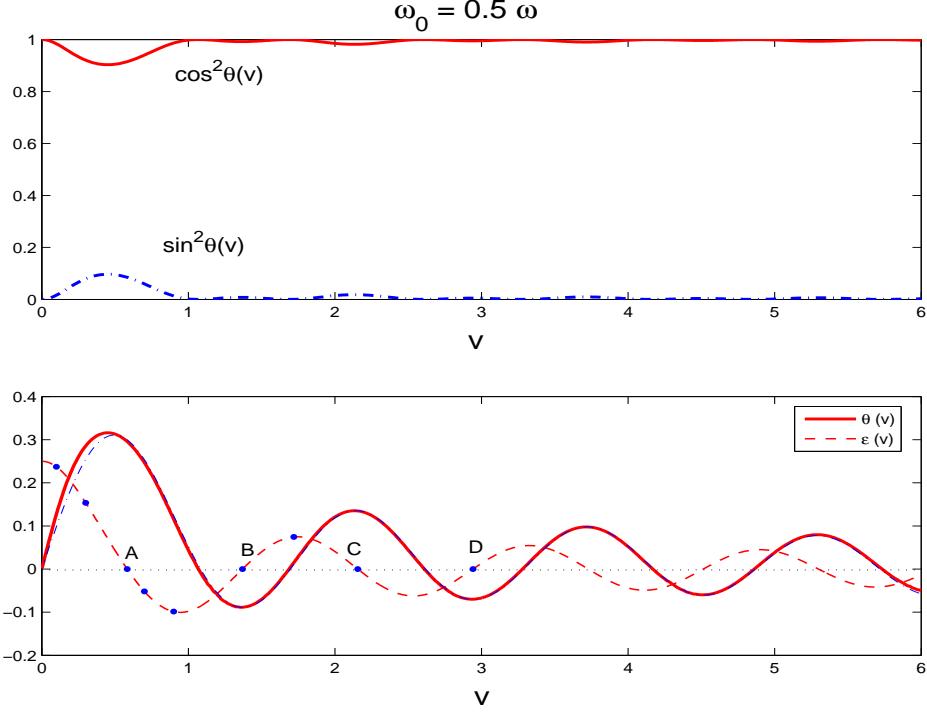
FIG. 7: The upper panel shows the functions $\cos^2(\theta(v))$ and $\sin^2(\theta(v))$, for $\tilde{\omega}_0 = 0.5$. At $t = 0$, the FES is given by $|\phi^{-\varepsilon}(0)\rangle = \cos\theta(v)|a\rangle + \sin\theta(v)|b\rangle$. The lower panel shows the functions $\theta(v)$ (solid line) and $\varepsilon(v)$ (dash line). The dash-dot line corresponds to the Struve function $\tilde{\omega}_0 \frac{\pi}{4} H_0(4v)$. Points A, B, C, D, correspond to the values of v for which DL occurs.
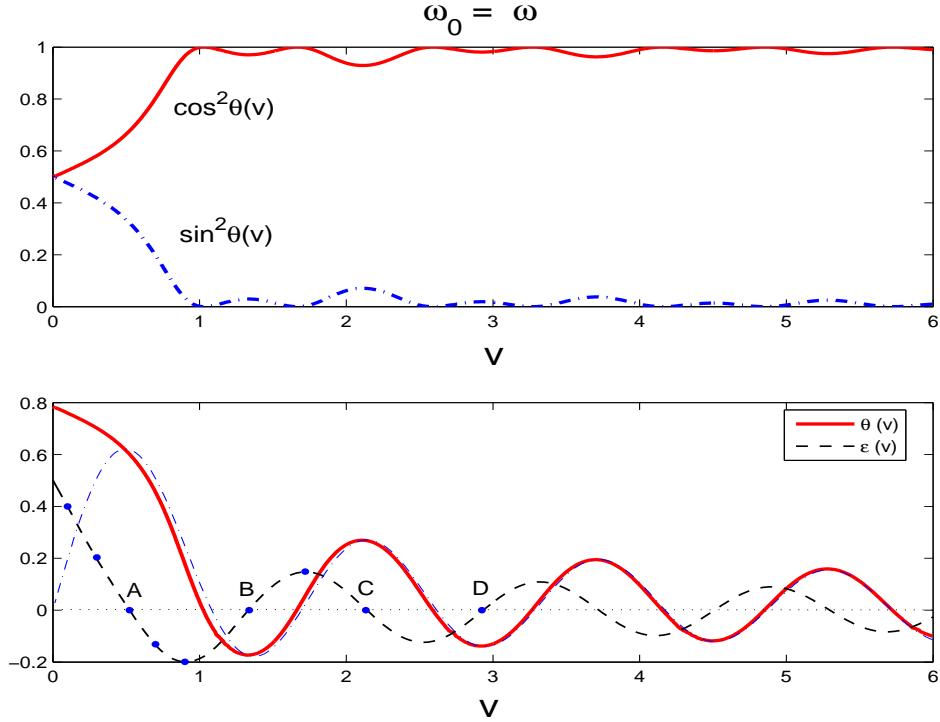
FIG. 8: Same as in Fig. 7. Here $\tilde{\omega}_0 = 1$.
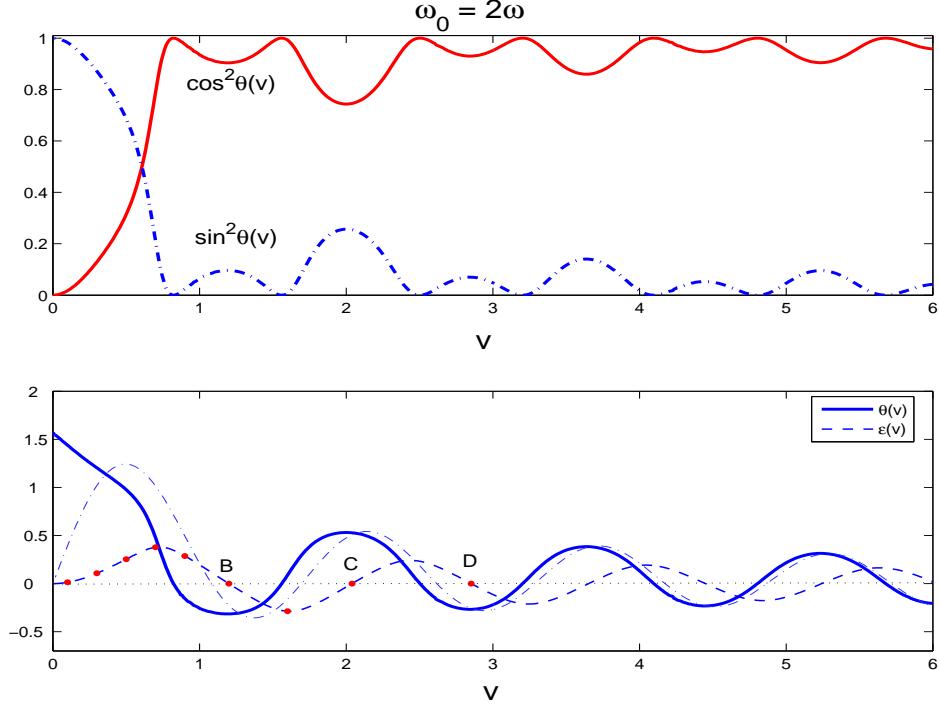
FIG. 9: Same as in Figs. 7,8. Here $\tilde{\omega}_0 = 2$.
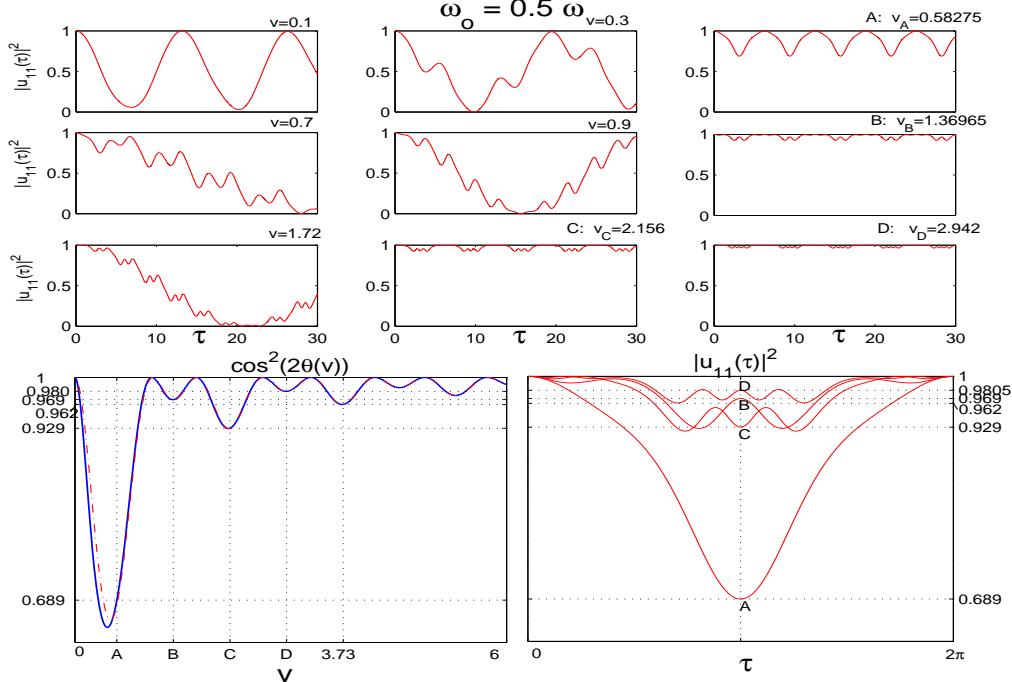
FIG. 10: The probability to remain in the initial state $|1\rangle$ as a function of time ($\tau = \omega t$), for 9 different values of the driving amplitude and for $\tilde{\omega}_0 = 0.5$. The lower panels show that the function $\cos^2(2\theta(v))$, at the DL points (A,B,C,D), gives a good approximation to the amount of localization P_l in this system. $P_l = \min(|u_{11}(\tau)|^2)$. In the lower left panel the function $\cos^2(2\tilde{\omega}_0 \frac{\pi}{4} H_0(4v))$ is shown with a dash-dot line for comparison.
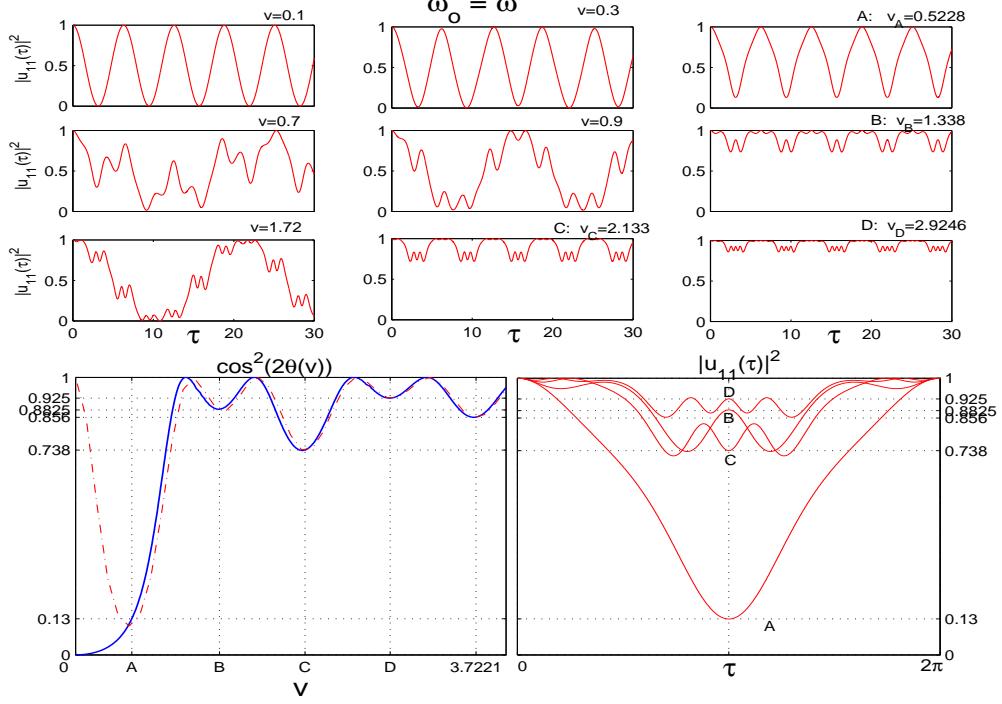
FIG. 11: FIG.11. As in Fig.10 . Here $\tilde{\omega}_0 = 1$.
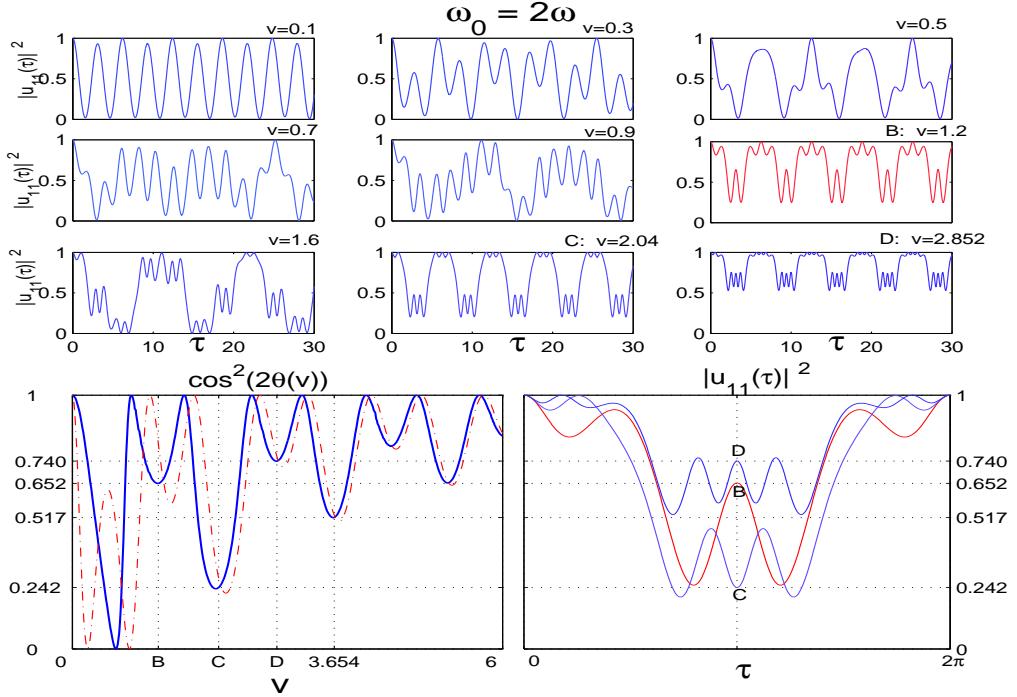
FIG. 12: As in Figs.10,11. Here $\tilde{\omega}_0 = 2$.
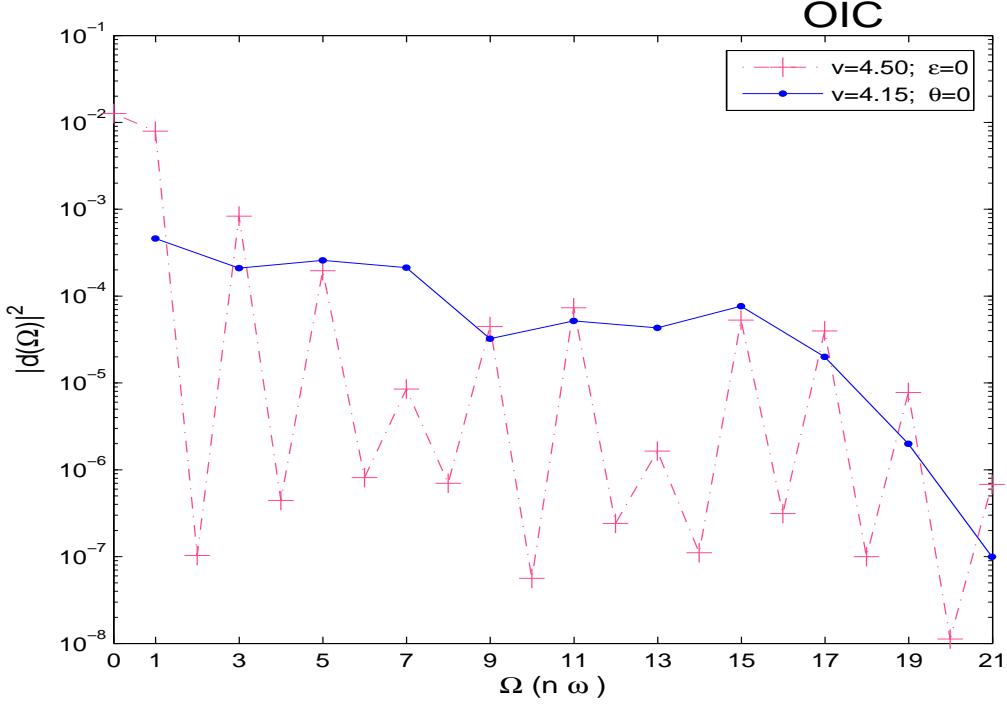
FIG. 13: The emission spectrum of the system, for the "Optical" Initial Condition (OIC) and for two values of the driving amplitude: $v = 4.5$ corresponds to a DL point and $v = 4.15$ gives $\theta(4.15) = 0$. The Fourier components of $\langle d(t) \rangle$ are connected with a continuous line for better visualization.
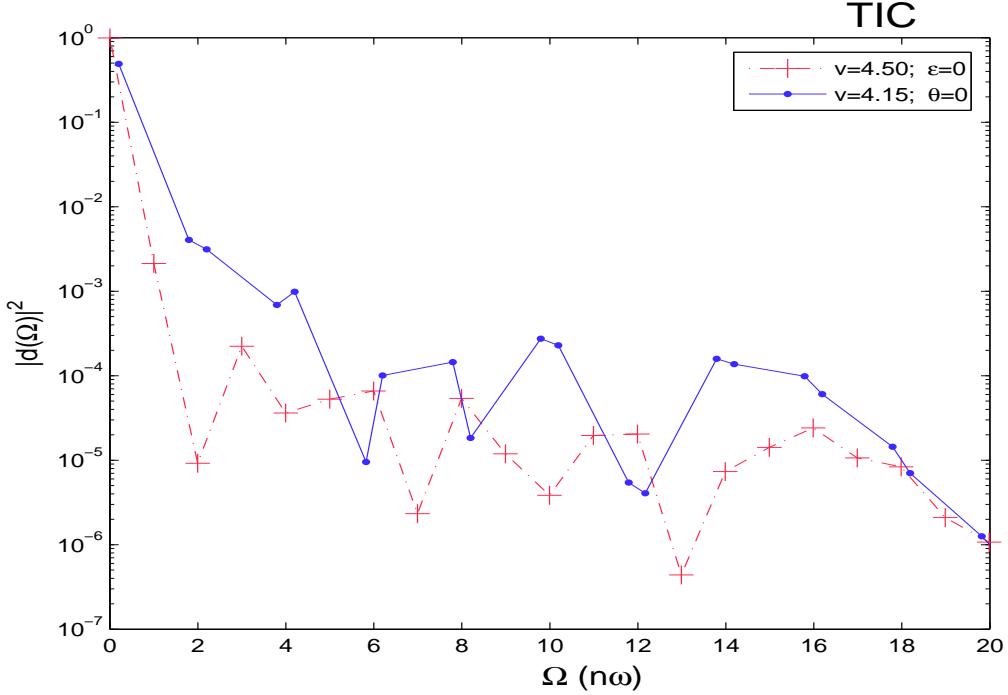

FIG. 14: Same as in Fig. 13. Here for "Tunneling" initial condition (TIC).
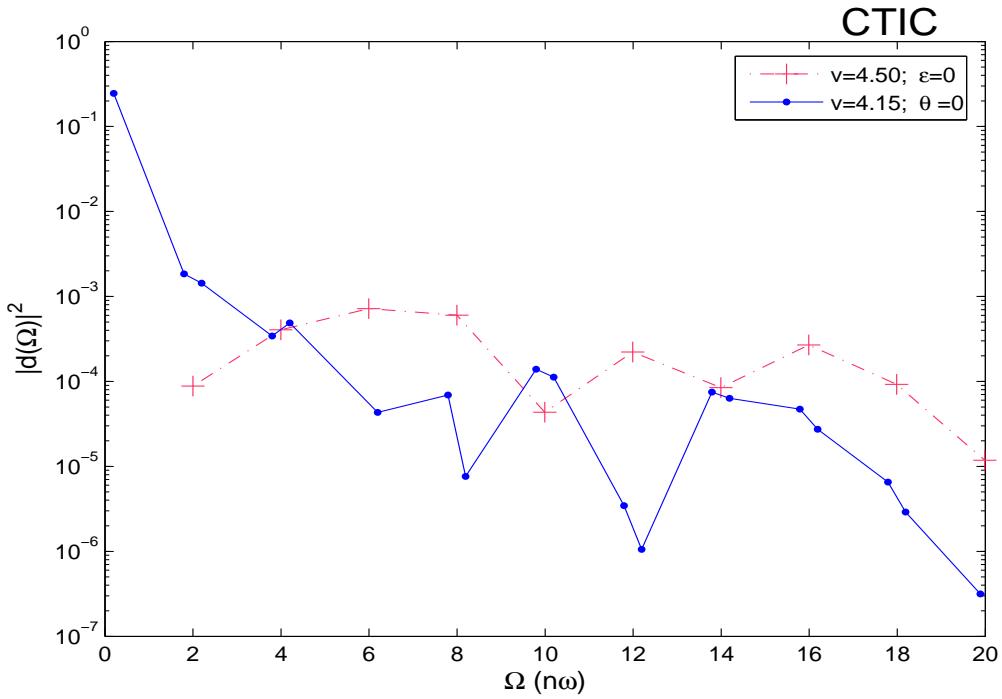
FIG. 15: Same as in Fig. 13,14. Here for "Complex Tunneling" Initial Condition (CTIC).